의학박사 학위논문

The Comprehensive Analysis of Genomic, Transcriptomic, and Pathologic Changes after Acquisition of Resistance to Immune Checkpoint Inhibitors

면역관문억제제에 대한 내성 획득 시 유전체, 전사체 및 병리학적 변화에 대한 통합적 분석

2020년 8월

서울대학교 대학원

의과대학 임상의과학과

유 신 혜

A thesis of the Degree of Doctor of Philosophy

면역관문억제제에 대한 내성 획득 시 유전체, 전사체 및 병리학적 변화에 대한 통합적 분석

The Comprehensive Analysis of Genomic, Transcriptomic, and Pathologic Changes after Acquisition of Resistance to Immune Checkpoint Inhibitors

August 2020

The Department of Clinical Medical Sciences

Seoul National University

College of Medicine

Shin Hye Yoo

Abstract

The Comprehensive Analysis of Genomic, Transcriptomic, and Pathologic Changes after Acquisition of Resistance to Immune Checkpoint Inhibitors

Shin Hye Yoo

The Department of Clinical Medical Sciences

The Graduate School

Seoul National University

Introduction: Immune checkpoint inhibitors (ICI) have emerging role in many cancer types. A certain proportion of patients who are treated with ICI have long-term durable response but finally progress and show acquired resistance to ICI. However, acquired resistance mechanism of ICI has not yet been elucidated. This study analyzed the changes after acquisition of resistance to ICI through genomic, transcriptomic, and pathologic analyses of

tumor samples of patients who were diagnosed as ICI-eligible type of cancer such as head and neck cancer or genitourinary cancer, in a comprehensive manner that takes into account both tumor-side (tumor-intrinsic) and immune-side (tumor-extrinsic)

Materials and Methods: The patients with immunogenic tumors (renal cell carcinoma, urothelial cell carcinoma, and head and neck squamous cell carcinoma) who received ICI between Dec 2013 and June 2017 were retrospectively analyzed. The patients who experienced response to ICI (complete response, partial response, or stable disease > 6 months) followed by progression and had available formalin-fixed paraffin-embedded tissues were enrolled. Whole exome sequencing, RNA sequencing and multiplex immunohistochemistry were performed on pre-treatment and resistant tumor samples. Tumor mutation burden, mutational signature and acquired resistance-associated somatic mutation were identified. Immune infiltrates, immune-related parameters such as immune checkpoints and immune activation markers, and the components of tumor microenvironment were evaluated. Evaluated parameters were classified into tumor-intrinsic and tumor-extrinsic – local immunity and systemic immunity.

Results: A total of 6 patients were analyzed. The median time to acquired resistance was 370 days (range, 210 to 739 days). Patient #1, who was diagnosed as human papillomavirus-positive head and neck squamous cell carcinoma, exhibited evident APOBEC-associated mutational signature in both pre-treatment and post-treatment samples. Resistance tumor tissue of the

patient harbored a missense mutation (E542K) in gene encoding *PI3KCA*, which can activate PI3K-Akt signaling pathway and may result in AR. In this patient, tumor mutational burden increased after ICI, whereas levels of cytotoxic CD8-positive T cells and immune checkpoints such as *PD-1*, *LAG3*, or *TIM3* were all decreased during AR. In patient #2, multiplex immunohistochemistry and RNA sequencing revealed the higher level of expression of alternative immune checkpoints including *PD-1*, *LAG3* and *TIM3* as well as CD8-positive tumor infiltrating lymphocytes were observed in post-treatment tumor than in pre-treatment tumor. Patient #3 showed a stop-gain mutation in gene encoding *AXIN2*, and patient #4 showed a frameshift deletion mutation in gene encoding *TET2*. In any of the patients, no significant mutations or copy number alterations of antigen presenting machinery or interferon-γ pathway were detected.

Conclusion: This study found that alternative immune checkpoint molecules were elevated after acquisition of resistance to ICI. Moreover, APOBEC-mediated *PIK3CA* mutagenesis might be a potential mechanism of acquired resistance.

Keywords: Acquired resistance, Mechanism, Immune checkpoint inhibitor, Next generation sequencing, immunohistochemistry, Programmed death-ligand 1, *PIK3CA*

Student number: 2017-31850

CONTENTS

LIST OF TABLES

LIST OF FIGURES

1. INTRODUCTION

Immune checkpoint inhibitors (ICI) are emerging as new treatments for different type of cancers. Programmed cell death-1 (PD-1) / programmed death-ligand 1 (PD-L1) axis is the most successful immune checkpoint to be targeted by ICI. PD-1 / PD-L1 blockades such as nivolumab or pembrolizumab have been approved for non-small cell lung cancer and melanoma first (1), and the use of PD-1 / PD-L1 blockades is expanding to other cancer types including genitourinary cancer (2) and head and neck squamous cell carcinoma (3). ICI, nowadays, is a crucial therapeutic option that should be integrated through the paradigm of treatment along with other therapeutics such as conventional chemotherapy or targeted agents, other modalities such as radiotherapy or surgery (4-8).

However, the response rate to ICI treatment alone still falls short of 20% despite numerous attempts to increase it. The number of studies exploring the biomarker for selection of adequate population is rapidly increasing (9-11). Although PD-L1 expression on tumor cell (12, 13) or tumor mutation burden (TMB) (14-16) is known as positive predictive biomarker for ICI response in some cancer types, there are still certain of patient groups that do not initially respond to ICI and shows acquired resistance. Moreover, the predictive role of tumor PD-L1 and TMB is inconsistent between cancer types (12, 15, 17). In sum, there is no definite biomarker for ICI responses yet, which means the

mechanism of resistance has been poorly studied yet (18, 19). So, exploring the mechanism of resistance to ICI has been the next important approach to maximize the effectiveness of ICIs.

Most of studies have focused on the mechanisms of primary resistance so far. However, little is known about the mechanism of acquired resistance, which is defined as progression after initial response for ICI (5). Unlike cytotoxic chemotherapy or targeted agent, ICIs are often characterized by long-term durable response in some patients (20-22), but they also would develop acquired resistance. Strategy for optimal management when acquired resistance occurs is not yet established, and unmet need for a guide in clinical practice is increasing. The most common mechanism of cytotoxic chemotherapy is mainly related to drug inactivation, increasing the release of drugs outside the cell, reducing the absorption of the drugs, inhibition of the cell death, changing the drug metabolism, *etc* (23, 24). Changing the chemotherapeutic agent targets by newly acquired genetic aberration is the most common resistance mechanism for targeted agents (25, 26). However, ICI acts by facilitating immune system in the patient to recognize cancer cells as non-self rather than by targeting or killing cancer cell directly. So, the mechanism of acquired resistance to ICI could differ from those to cytotoxic chemotherapy or targeted agents (27).

To date, some mechanisms of acquired resistance have been observed in previous studies. Based on the mechanisms of actions of ICIs, hypothetical mechanism of resistance to ICI can appertain to any of three

categories, as suggested by a previous review article (28): 1) insufficient generation of anti-tumor T cells, 2) inadequate function of tumor-specific T cells, or 3) impaired formation of T cell memory. The defect of antigen presenting machinery such as loss of heterozygosity of β2-microglobulin gene (29-31), and change of neo-antigens during ICI treatment (32) can go for the first category. For the second category, loss-of-function mutation of Janus Kinase 1 (*JAK1*) and Janus Kinase 1 (*JAK2*) (29), can give rise to acquired resistance in clinics. In addition, upregulations of other immune checkpoint molecules were thought to be another acquired resistance mechanism through T cell exhaustion (33, 34).

However, a few limitations are noted in those previous studies. First, the studies were mostly limited to patients with non-small cell lung cancer or malignant melanoma. Second, the studies included only a small number of patients because the prevalence of acquired resistance is little (18, 35), and it is challenging to achieve sufficient tissues and blood samples for genomic, transcriptomic, and pathologic analysis. Finally, such acquired resistance mechanisms were observed only in some patients (18). These might not fully represent why the remaining patients without clear resistance mechanism show acquired resistance. This insists that previously reported mechanisms of acquired resistance to ICI could not be generalized to the patients with different cancer types and that more cases exploring the acquired resistance mechanism are needed. Moreover, the comprehensive analysis in a scope

including tumor side and immune side should be performed.

Therefore, this study aimed to analyze the changes after acquisition of resistance to ICI through genomic, transcriptomic, and pathologic analyses of tumor samples of patients who were diagnosed as immunogenic tumors in a comprehensive manner considering both tumor-side (tumor-intrinsic) and immune-side (tumor-extrinsic).

2. MATERIALS AND METHODS

2.1. Patient population

Medical records of patients with immunogenic tumors (renal cell carcinoma (RCC), urothelial cell carcinoma (UCC), or head and neck cancer) who treated with ICI (PD-1 / PD-L1 blockade single or combination) in Seoul National University Hospital between Dec 2013 and June 2017 were retrospectively reviewed. Among them, patients 1) > 19 years or older, 2) who showed acquired resistance, defined as experiencing response to ICI (complete response, partial response, or stable disease > 6 months, assessed by the Response Evaluation Criteria in Solid Tumors guideline, version 1.1 (36)) followed by progression, and 3) who had available enough pre-treatment and post-treatment (resistant) tumor tissues and matched peripheral blood mononuclear cells (PBMC) were included. A total of 6 patients were enrolled. Baseline patient characteristics (including age, sex, histologic differentiation, location of tumor, and stage) and treatment outcomes were retrospectively obtained from medical records. The study protocol was reviewed and approved by the Institutional Review Board of the Seoul National University Hospital (approval no. H-1809-144-978). The study was conducted in accordance with the Principles of the Declaration of Helsinki.

2.2 Tissue preparation and multiplex immunohistochemistry (IHC)

Specimens from patients were formalin-fixed and paraffin-embedded (FFPE). All human FFPE tissue samples were obtained from the archive of the Department of Pathology in Seoul National University Hospital. Two pathologists (SHK and JMK) reviewed specimens and designated representative tumor regions identified by hematoxylin and eosin (H&E) stained sections. Quantitative multiplex immunohistochemical staining was conducted using PerkinElmer Opal kit (Perkin-Elmer, Waltham, MA, USA). One pathologist (JMK) marked representative tumor regions (tumor marking) on the electronic image file. Four μm of FFPE tissue sections was cut by rotation microtome. Following being heated at least for 1 hr in a dry oven at 60°C and deparaffinization with 100% xylene, the sections were rehydrated. Antigen retrieval was performed with Bond Epitope Retrieval 2 (#AR9640, Leica Biosystems, Newcastle, UK) in a pH 9.0 solution for 30min. 3% H2O2 blocking solution followed by Dako antibody diluent was used for blocking. Multiplex immunofluorescence staining was performed with a Leica Bond Rx™ Automated Stainer (Leica Biosystems, Newcastle, UK). The first primary antibodies for cytokeratin (CK) (NBP2-29429, NOVUS, dilution 1:500) were incubated for 1 hour in a humidified chamber at room temperature, and the OpalTM Polymer HRP Ms+Rb kit (ARH1001EA,

Perkin-Elmer, MA, USA) was used for detection. Visualization of CK was accomplished using Opal 780 TSA Plus (dilution 1:25), after which the slide was treated with Bond Epitope Retrieval 1 (#AR9961, Leica Biosystems, Newcastle, UK) for 20 min to remove bound antibodies before the next step in the sequence. In a serial fashion, cluster of differentiation 3 (CD3) (790-4341, Ventana, dilution 1:300, Perkin-Elmer, Opal 480 TSA Plus 1:150), PD-L1 (13684S, Cell Signaling, dilution 1:300, Perkin-Elmer, Opal 690 TSA Plus 1:150), PD-1 (ab137132, Abcam, dilution 1:500, Perkin-Elmer, Opal 520 TSA Plus 1:150), Lymphocyte-activation gene 3 (LAG3) (LS-C18692, LSBio, dilution 1:100, Perkin-Elmer, Opal 570 TSA Plus 1:150), T-cell immunoglobulin and mucin-domain containing-3 (TIM3) (45208S, Cell Signaling, dilution 1:200, Perkin-Elmer, Opal 620 TSA Plus 1:150) was stained. In another panel, cluster of differentiation 4 (CD4) (ab133616, Abcam, dilution 1:200, Perkin-Elmer, Opal 480 TSA Plus 1:150), cluster of differentiation 8 (CD8) (HCA1817, Bio-rad, dilution 1:300, Perkin-Elmer, Opal 520 TSA Plus 1:150), Human Leukocyte Antigen (HLA) class I (ab70328, Abcam, dilution 1:40000, Perkin-Elmer, Opal 620 TSA Plus 1:150), cluster of differentiation 86 (CD86) (91882S, Cell Signaling, dilution 1:300, Perkin-Elmer, Opal 690 TSA Plus 1:150) and cluster of differentiation 163 (CD163) (ab182422, Abcam, dilution 1:500, Perkin-Elmer, Opal 570 TSA Plus 1:150) was stained. Nuclei were subsequently visualized with nuclear spectral elements (4′,6-diamidino-2-phenylindole, DAPI), and the section was coverslipped using HIGHDEF® IHC fluoromount (ADI-950-260-0025, Enzo,

USA). The PerkinElmer Vectra 3.0 Automated Quantitative Pathology Imaging System (Perkin-Elmer, MA, USA) was used for scanning slides, and images were analyzed using the inform 2.2 software and TIBCO Spotfire™ (Perkin-Elmer, MA, USA). Each cell was identified by detecting DAPI. Using the cell segmentation tool by the InForm image analysis software, all the immune cell populations from each panel was quantified and designated as positive or negative for each antibody. The numbers of CK, CD3, PD-L1, PD-1, LAG3, TIM3, CD4, CD8, HLA class I, CD86, and CD163 positive cells were counted in each slide. I also analyzed the data for CD3, CD4, CD8, PD-1, LAG3 and TIM3 in cells with lymphocyte-range of diameters (5 to 15 um) and the data for CD86 and CD163 in cells with macrophage-range of diameters (15 to 25 um). To characterize the expression of the markers on tumor cells, PD-L1 and HLA class I on CK-positive cells were used for analysis.

2.3. DNA and RNA extraction process

Genomic deoxyribonucleic acid (DNA) and ribonucleic Acid (RNA) were isolated from a-10μm thick section of FFPE tumor tissue using a Maxwell® RSC DNA/RNA FFPE kit (Promega, Madison, WI, USA). Genomic DNA from peripheral blood was extracted using the Maxwell® RSC Blood DNA kit (Promega). Genomic DNA and RNA concentration and purity were measured using a EON (BioTek., Winooski, VT, USA) and a Qubit 2.0

Fluorometer (Life Technologies Inc., USA).

2.4. Whole Exome Sequencing (WES) and data analysis

High quality genomic DNA in each sample was sheared with an S220 ultra-sonicator (Covaris, USA), and library was constructed with the SureSelect XT Human All Exon 50Mb and SureSelect XT reagent kit, HSQ (Agilent Technologies), according to the manufacturer's protocol. The exome libraries were sequenced on the HiSeq 2500 platform (Illumina, USA) and prepared via genomic DNA shearing, end-repair, A-tailing, paired-end adaptor ligation and amplification. The library was also hybridized with bait sequences, purified and amplified with a barcode tag. Quality and quantity of the library were evaluated using a 2200 TapeStation Instrument and Qubit 2.0 Fluorometer, respectively. The exome library was sequenced using the 10-bp paired-end mode of the TruSeq Rapid PE Cluster kit and the TruSeq Rapid SBS kit (Illumina, USA). Sequencing depth as 200x for tumor tissue and 80x for peripheral blood mononuclear cells was planned. Sequencing characteristics and information were described in **Table 1**.

Table 1. Whole exome sequencing quality and information

Sample ID	Total read	%GC	%N	%Q20	%Q30	Mapping rate%	On-target rate%	On-target depth
#1-blood	47,250,856	47.17%	0.05%	95.09%	90.63%	96.01%	66.21%	49.16
#1-pre	133,864,160	51.96%	0.05%	95.99%	91.98%	83.52%	68.67%	152.72
#1-post	149,251,190	52.33%	0.04%	96.10%	92.32%	87.56%	59.48%	145.29
#2-blood	45,368,046	48.28%	0.09%	97.88%	95.97%	97.64%	65.89%	48.16
#2-pre1	112,229,928	48.69%	0.04%	98.25%	96.71%	76.94%	53.22%	99.54
#2-pre2	100,954,896	50.03%	0.10%	98.16%	96.48%	93.65%	75.13%	127.33
#2-post	124,882,528	55.72%	0.05%	95.66%	91.38%	84.04%	59.74%	124.55
#3-blood	44,035,340	49.66%	0.10%	97.82%	95.89%	97.46%	75.87%	53.87
#3-pre	107,468,288	50.93%	0.09%	98.27%	96.65%	83.08%	65.27%	118.12
#3-post	106,341,600	51.01%	0.09%	98.22%	96.59%	68.41%	47.75%	82.09
#4-blood	40,014,512	49.63%	0.10%	97.86%	95.91%	97.81%	77.50%	50.19
#4-pre	126,577,470	50.13%	0.05%	98.08%	96.30%	52.72%	32.54%	64.89
#4-post	107,385,452	49.25%	0.09%	98.30%	96.72%	88.22%	73.27%	131.66
#5-blood	52,499,440	47.19%	0.05%	95.23%	90.78%	95.10%	66.47%	54.62
#5-pre	142,327,880	51.03%	0.05%	94.58%	89.38%	81.95%	61.99%	143.09
#5-post	145,424,824	52.68%	0.05%	95.55%	91.25%	75.91%	59.48%	142.48
#6-blood	58,332,668	47.01%	0.05%	95.23%	90.79%	92.46%	63.76%	58.39
#6-pre1	115,773,210	49.13%	0.04%	96.81%	93.66%	91.98%	26.08%	49.98
#6-pre2	90,324,218	47.31%	0.05%	96.50%	93.27%	95.54%	16.59%	24.79
#6-post	112,409,210	57.37%	0.05%	95.48%	90.98%	91.58%	75.47%	139.9

The GRCh37 human reference genome was used to align the sequencing reads via the Burrows-Wheeler Aligner (BWA)-0.7.10 (37). Read sorting and polymerase chain reaction (PCR) duplicate removal was performed by Picard-tools-1.124 (http://broadinstitute.github.io/picard/). Genome Analysis Tools Kit (GATK)-3.7 (38) was used for performing data pre-processing including local realignment around indels and base quality score recalibration. Mutect2 was used to detect somatic single nucleotide polymorphisms and Indels using tumor and matched normal blood. Annovar (39) was used to annotate variants. The following criteria were used to reduce false positive variants: 1) Mutect2 filter=PASS. 2) Significant single nucleotide polymorphism was defined as Alt allele depth ≥ 4 and Alt allele frequency ≥ 0.03, and significant Indel as Alt allele depth ≥ 4 and Alt allele frequency ≥ 0.05. Moreover, exonic and splicing variants were only retained. TMB was measured by the number of somatic single nucleotide variants and indel mutations that passed the set criteria per megabase in the coding region. The synonymous as well as nonsynonymous mutations were included (40). Signature analysis of mutational processes was carried out using deconstructSigs R package (41).

In order to identify more significant variants in the somatic mutation profile, synonymous variants and common variants with allele frequency > 1% in 1000G, ExAC, and ESP databases were removed. Additionally, variants that predicted to be functionally neutral by CADD (Phred score < 15) or by

both SIFT (pred="T") and PolyPhen-2 (pred="B") according to Annovar annotation were also excluded. For identifying acquired resistance-associated somatic mutations, which were present only in post-treatment samples, I followed a re-checking process, which entailed examining whether the somatic mutations found in a post-treatment sample were present in Mutect2 raw result without additional filtering of the pre-treatment sample. A mutation diagram ("lollipop plot") of phosphatidylinositol-4,5-bisphosphate 3-kinase catalytic subunit alpha (*PIK3CA*) variant was generated with MutationMapper (42, 43). Copy number variations were identified by EXCAVATOR2 (44) and CNVkit (45).

2.5. mRNA Sequencing and data analysis

Library for RNA sequencing (RNA-seq) was constructed using a TruSeq RNA Exome (Illumina, USA). A reverse transcription reaction with poly (dT) primers was performed with isolated RNA using Super-ScriptTM II Reverse Transcriptase (Invitrogen/Life Technologies, USA), according to the manufacturer's protocol. An RNA-seq library was prepared via complementary DNA amplification, end-repair, 3′ end adenylation, adapter ligation, and amplification. Library quality and quantity were measured using the Bioanalyzer and Qubit. Sequencing of the RNA library was carried out using the 100-bp paired-end mode of the TruSeq RNA Exome (Illumina, USA).

The paired-end sequencing reads were aligned to the hg38 reference genome using STAR aligner-2.6.0 (46) and gene expression values were quantified by RNA-Seq by Expectation-Maximization-1.3.1 (47). A total of 18,161 coding genes were analyzed for transcript abundance and poorly expressed genes were eliminated based on the criteria of a maximum read count > 20 for all samples. Read counts were normalized using the fragments per kilobase million (FPKM) normalization method.

Tumor purity and immune scores based on RNA-seq were calculated using Estimation of STromal and Immune cells in MAlignant Tumor tissues using Expression data (ESTIMATE) (48). Fractions of immune-associated cell types were calculated by CIBERSORT (49) using RNA-seq expression profiles.

Genes with average FPKM of two samples ≥ 5 and $\log_2$ (fold change of FPKM) ≥ 2 were considered to be differentially expressed genes between pre-treatment and post-treatment sample for each case. DAVID bioinformatics resources (DAVID, https://david.ncifcrf.gov/) (50) was utilized for performing pathway enrichment analysis using only genes with an average FPKM of two samples ≥ 20 as differentially expressed gene for input. Single-sample gene set enrichment analysis (ssGSEA) was also utilized for performing pathway enrichment analysis (51).

2.6. Acquisition of gene sets for profile identification

I regarded known cancer genes from the cancer gene census (52) as cancer-associated genes. I further inferred oncogenic variants in cancer-associated genes based on COSMIC (Occurrence ≥ 3) (52), ClinVar (CLNSIG="Pathogenic") (53), and OncoKB (54). I examined the profiles of multiple gene sets likely to be involved in AR mechanism such as immune checkpoint (HisgAtlas, http://biokb.ncpsb.org/HisgAtlas/index.php/Home/Browse/) (55), cytolytic activity (56), antigen presenting machinery (KEGG, https://www.genome.jp/dbget-bin/www_bget?hsa04612) (30, 57), interferon-γ (IFN-γ) signaling pathway (58), and IFN-γ signature (59).

2.7. Statistical analysis

Overall survival (OS) was defined as the time from initiating ICI until death, and the progression-free survival (PFS) was defined as the time from the initiating ICI to disease progression or any cause of death.

3. RESULTS

3.1. Baseline clinical characteristics

A total of six patients showing acquired resistance participated in paired WES analysis, RNA-seq analysis and multiplex IHC analysis (**Figure 1**). An example of clinical course of a patient is depicted in **Figure 2**. Patient #2, a 41-year-old male with clear cell RCC was given right nephrectomy at diagnosis and right lung metastatectomy after 2 years when the disease was recurred in lung. Because he had very slowly progressive disease, he initiated anti-PD-L1 monotherapy 14 months after one more resection of the lung metastases without preceding chemotherapy. He achieved stable disease after 3 cycles of the treatment. After about 15 months of the treatment, mass lesions adjacent to the seventh rib increased, so wedge resection of right upper and lower lobes and video-assisted thoracoscopic rib excision were conducted.

The baseline clinical characteristics of the study population are shown in **Figure 3** and **Table 2**. Two patients (#3 and #4) showed partial response, and four (#1, #2, #5 and #6) showed stable disease. The median time to acquired resistance was 370 days (range, 210 to 739 days). The patients comprised a case of head and neck squamous cell carcinoma (HNSCC) (#1), a case of nasopharyngeal carcinoma (#3), three cases of clear cell RCC (#2, #4, and #6), and a case of invasive UCC of the bladder (#5).

Three patients received single ICI and three received combination treatment. Tumor samples from patient #1, #4 and #5 were obtained just before the initiation of ICI, whereas those from patient #2, #3 and #6 were obtained before an earlier course of therapy. Clinical characteristics of tumor samples are described in **Table 3**.

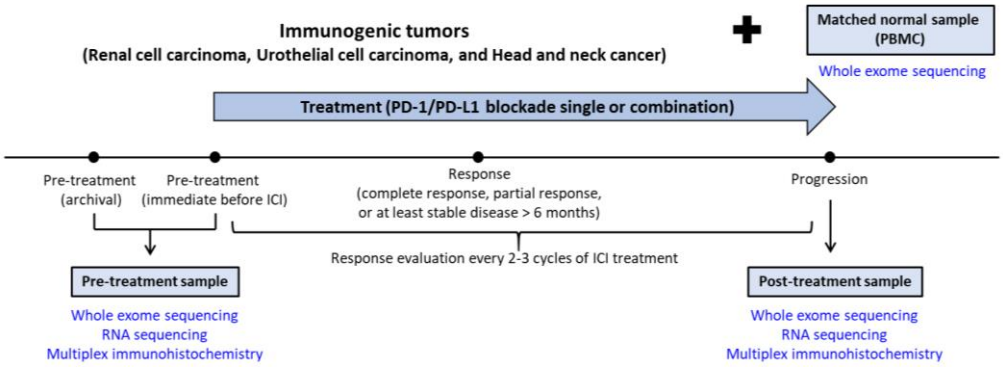

Figure 1. Study flow and analytic process of the patients showing acquired resistance to ICIs.

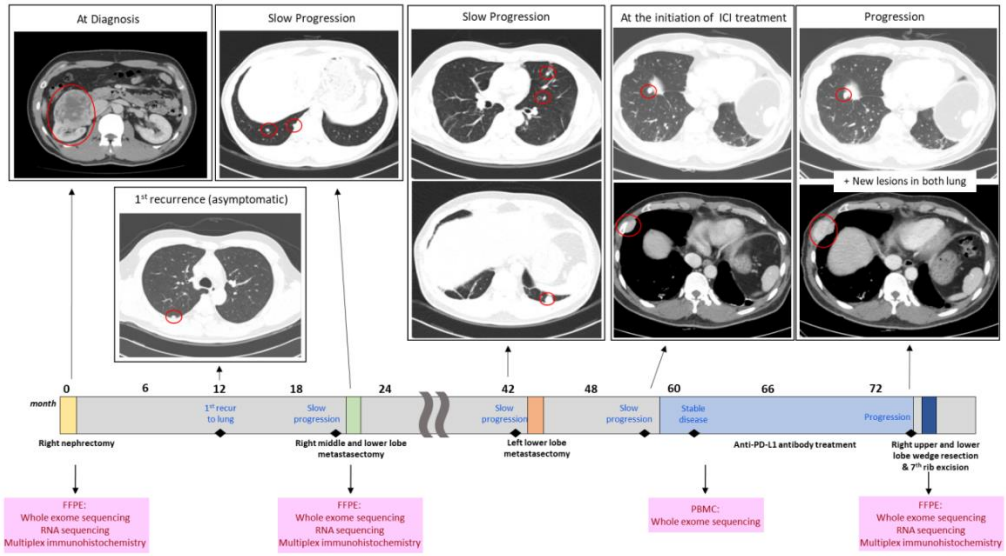

Figure 2. Clinical course with radiologic images and tissue collection timepoints for whole exome sequencing, RNA sequencing, and multiplex immunohistochemistry in a patient with renal cell carcinoma (patient #2).

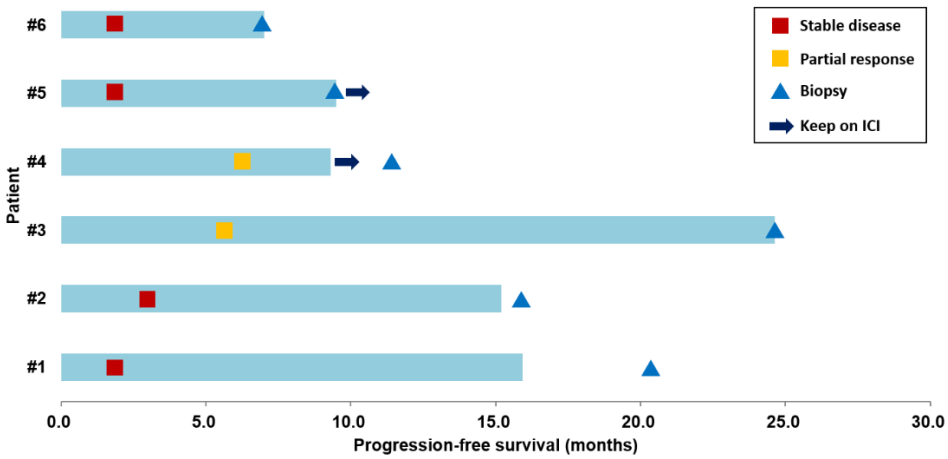

Figure 3. Swimmer's plot indicating progression-free survival, best response, and the time to acquisition of tissue at acquired resistance to ICI.

Table 2. Baseline clinical characteristics of patients

Patient No.	Age /Sex	Diagnosis	ECOG PS at baseline	Tumor burden*	No. of Prior systemic therapy	Type of ICIs	Response	PFS	OS	Treatment duration
#1	59/M	Tonsillar cancer (HPV+)	1	15mm	1	α-PD-1+ α-CTLA-4	SD	15.9mo	23.1mo†	15.9mo
#2	41/M	ccRCC	0	39mm	0	α-PD-L1	SD	15.2mo	36.9mo†	15.2mo
#3	19/M	Nasopharyngeal cancer	1	60mm	1	α-PD-1	PR	24.6mo	60.2mo	23.6mo
#4	63/M	ccRCC	1	17mm	0	α-PD-L1+α-VEGF	PR	9.3mo	22.2mo	19.4mo
#5	56/M	UCC (bladder)	1	40mm	0	α-PD-L1	SD	9.5mo†	28.7mo†	28.7mo
#6	46/M	ccRCC	1	73mm	3	α-PD-L1+MEK inhibitor	SD	7mo	20.1mo†	6.1mo

* Tumor burden was defined as baseline tumor size, which was calculated by summation of the largest diameter of the target lesions per RECIST version 1.1 (60).

† Ongoing at census

Abbreviations: No., number; ECOG, Eastern Cooperative Oncology Group; PS, performance status; ICI, immune checkpoint inhibitor; PD, progression; PFS, progression-free survival; OS, overall survival; M, male; HPV, human papillomavirus; ccRCC, clear cell renal cell carcinoma, UCC, urothelial cell carcinoma; α-, anti-; PD-1, programmed cell death-1; PD-L1, programmed death-ligand 1; CTLA-4; cytotoxic T-lymphocyte–associated antigen 4; VEGF; vascular endothelial growth factor; MEK, mitogen-activated protein kinase kinase; SD, stable disease; PR, partial response;

Table 3. Clinical information of tumor samples

Sample ID	Site	Type of specimen	Clinical scenario*
#1-pre	Lymph node	Surgical, FFPE	Pre-treatment, recent
#1-post	Spine	Surgical, FFPE	Post-treatment, new lesion
#2-pre1	Kidney	Surgical, FFPE	Pre-treatment, remote
#2-pre2	Lung	Surgical, FFPE	Pre-treatment, remote
#2-post	Lung	Surgical, FFPE	Post-treatment, in situ relapse and new lesion
#3-pre	Brain	Surgical, FFPE	Pre-treatment, remote
#3-post	Lung	Surgical, FFPE	Post-treatment, in situ relapse
#4-pre	Kidney	Surgical, FFPE	Pre-treatment, recent
#4-post	Bone (T12)	Surgical, FFPE	Post-treatment, new lesion
#5-pre	Bladder	Surgical, FFPE	Pre-treatment, recent
#5-post	Bladder	Surgical, FFPE	Post-treatment, in situ relapse
#6-pre1	Bone (femur)	Surgical, FFPE	Pre-treatment, remote
#6-pre2	Kidney	Surgical, FFPE	Pre-treatment, remote
#6-post	Adrenal gland	Surgical, FFPE	Post-treatment, in situ relapse

Abbreviations: ICI, immune checkpoint inhibitor; FFPE, Formalin-Fixed Paraffin-Embedded; PD, progressive disease;

*If the pre-treatment tumor sample was obtained between the last treatment before ICI and ICI treatment, it was indicated as ‘recent’. Other cases were marked as ‘remote’. For post-treatment tumor samples, site of PD (new lesion or in situ relapse) was described.

3.2. Tumor-intrinsic: from the perspective of tumor

3.2.1. Tumor mutational burden

TMB has been known to be associated with treatment response to ICI and used as predictive biomarker (14). In non-small cell lung cancer patients who received ICI, decreased TMB with neo-antigen burden was associated with acquired resistance (32), so I analyzed the number of somatic mutation and TMB from processed whole exome sequencing data.

The median numbers of tumor purity before and after ICI treatment were 0.63 and 0.61, respectively (range, 0.47 to 0.73; 0.48 to 0.79, respectively) (**Figure 4**). The median somatic TMB in the pre-treatment samples was 3.31 (range 0.74 to 5.5). Compared to the TMB in the same cancer types from previously reported data (40), the somatic TMB in the pre-treatment samples was low, except for patient #1 and #3. In patient #2 and #3, the somatic TMB decreased after acquisition of resistance. Increased TMB was found only in the post-treatment sample of patient #1 (**Figure 5**).

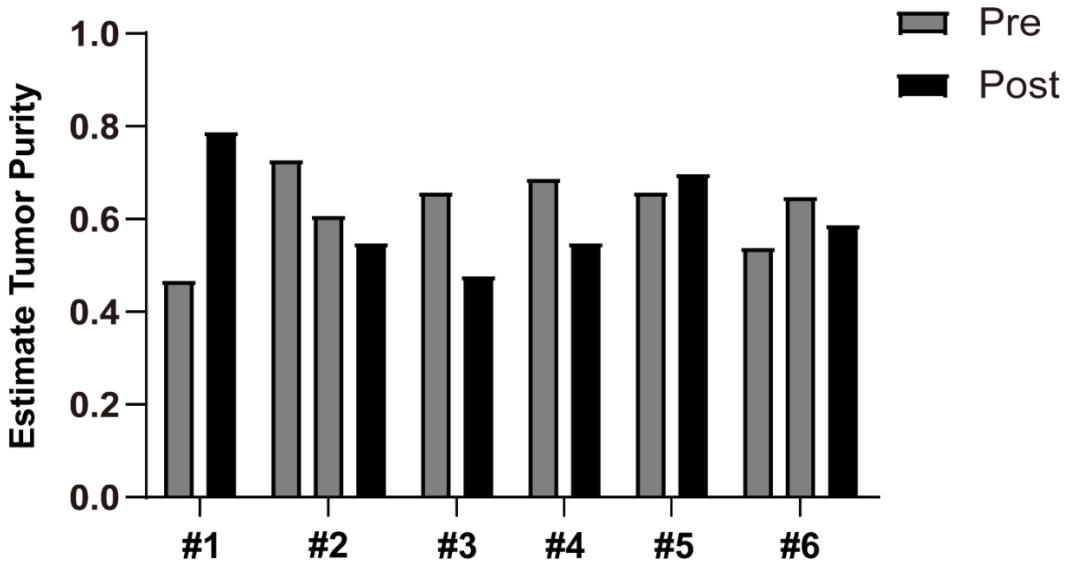

Figure 4. Tumor purity identified by Estimation of STromal and Immune cells in MAlignant Tumor tissues using Expression data.

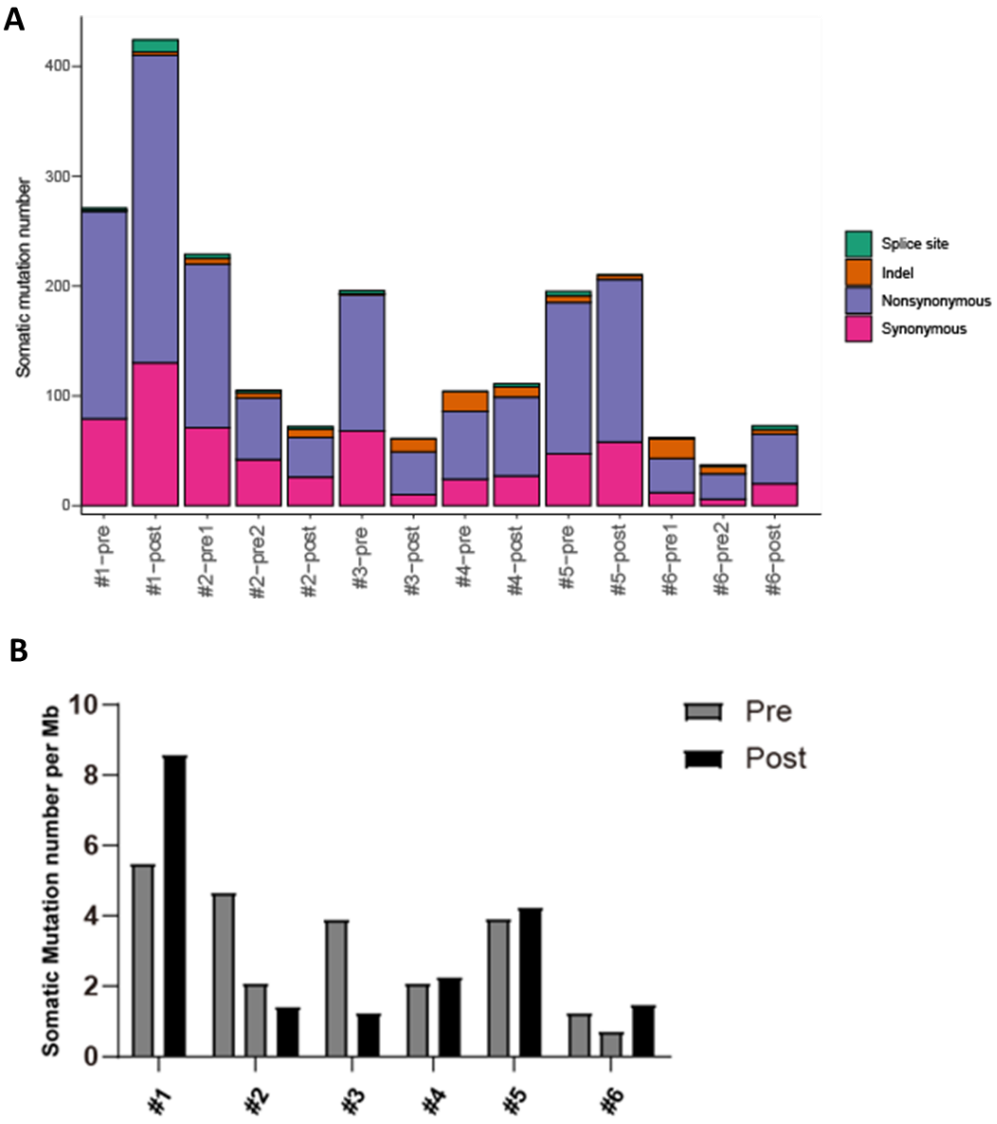

Figure 5. The number of somatic mutation and tumor mutation burden of patients with acquired resistance to ICIs. (A) The number of somatic mutation. (B) Tumor mutation burden as somatic mutation number per megabase (Mb).

3.2.2. Mutational signature

Signatures which were associated with smoking (61), mismatch repair (62, 63), or the apolipoprotein B mRNA editing catalytic polypeptide-like (APOBEC) mutations (64) have been reported to be associated with treatment response to ICIs. Signature related to mismatch repair deficiency is associated with improved ICI response owing to hyper-mutated phenotype by increased TMB.

In this study, the analysis of the mutation spectrum of the pre-treatment samples showed prominent C>T transitions, as has been demonstrated in many solid cancers (**Figure 6A**). The predominant mutational signatures of the post-treatment samples were mostly retained after ICI treatment, with the exception of 2 paired cases (patient #3 and #4) (**Figure 6B**), similar to the results from a report of non-small cell lung cancer patients (30). Patient #1 and #5 exhibited a mutational signature (signature 13) rich in both C>T transitions and C>G transversion at TC dinucleotides, suggestive of being associated with APOBEC mutations (65), which was also retained both in pre-treatment and resistant samples.

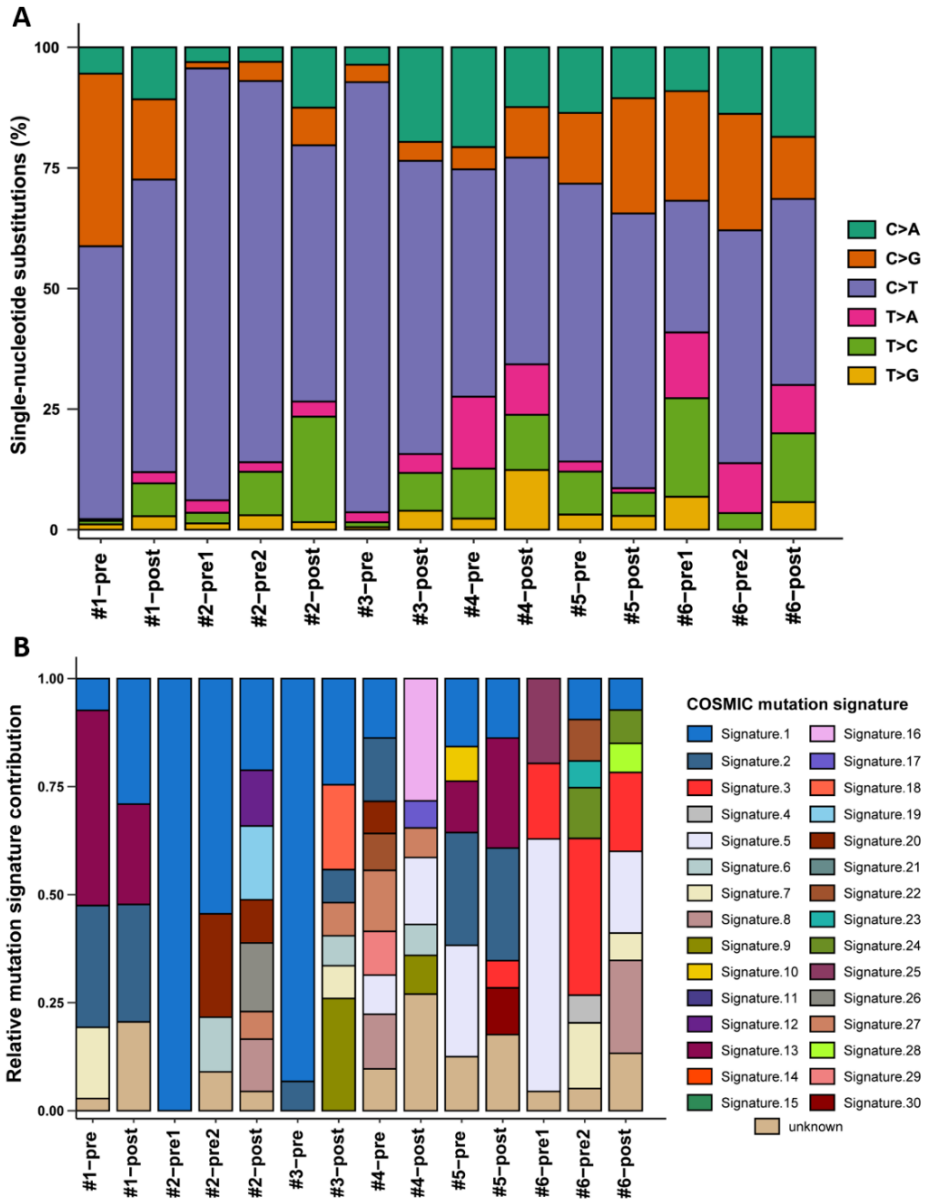

Figure 6. Mutation frequency and signatures. (A) The frequency of mutation spectrum. (B) Mutation signature.

3.2.3. Oncogenic signaling pathways

To investigate the aberration of oncogenic signaling pathway that might be associated with resistance to ICI, I analyzed the aberration of tumor cell genes including oncogenes and tumor suppressor genes, which occurred only in resistant samples. Any of acquired resistance-associated somatic mutations were not overlapped between patients (**Figure 7 and Figure 8**).

3.2.3.1. Activation of PI3K-Akt signaling pathway

Alteration of phosphatase and tensin homolog (*PTEN*) through deletion or inactivating mutations has been frequently found in different types of cancer (66, 67) and has been reported to be associated with immune escape (67-70). However, I could not find any evidence of *PTEN* alteration through mutation and expression data (**Figure 8 and Figure 9**). Instead, I identified that post-treatment sample of patient #1 had an E542K missense mutation that lies within the PIK helical domain of the Pik3ca protein (variant allele frequency, 34.1%) (**Figure 10A**). This mutation has been known as hotspot mutation, which is commonly found in breast cancer and colorectal cancer (71, 72). Integrative Genomics Viewer plot displayed that the frequency of the *PI3KCA* E542K mutation was observed at higher levels in the resistance sample than in the pre-treatment sample (**Figure 10B**). By pathway enrichment analysis, enrichment of PI3K-Akt signaling pathway was found in the post-treatment sample of #1 (**Figure 11**).

ETS variant transcription factor 1 (*ETV1*) is known to be related to Akt

signaling as well (73), and a missense mutation (R188H) in gene encoding ETV1 was found in post-treatment sample of patient #5 (**Figure 7**). However, change in PI3K-Akt signaling pathway was not observed in this patient.

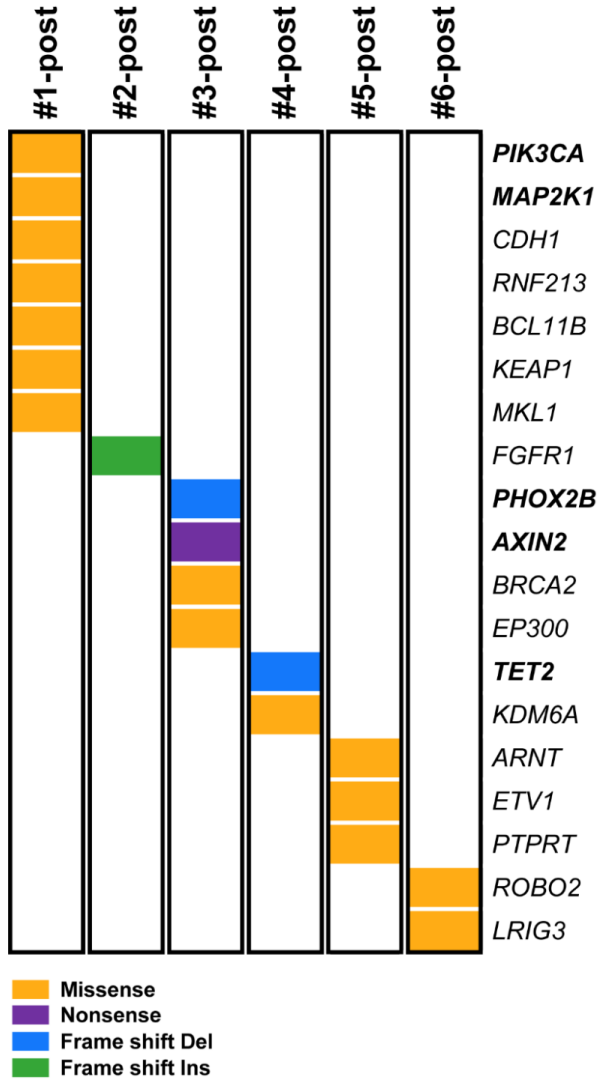

Figure 7. Acquired resistance-associated somatic mutation profiles (post-treatment only) of cancer genes.

Variants in genes marked with bold font mean oncogenic variants inferred from COSMIC, ClinVar, and OncoKB.

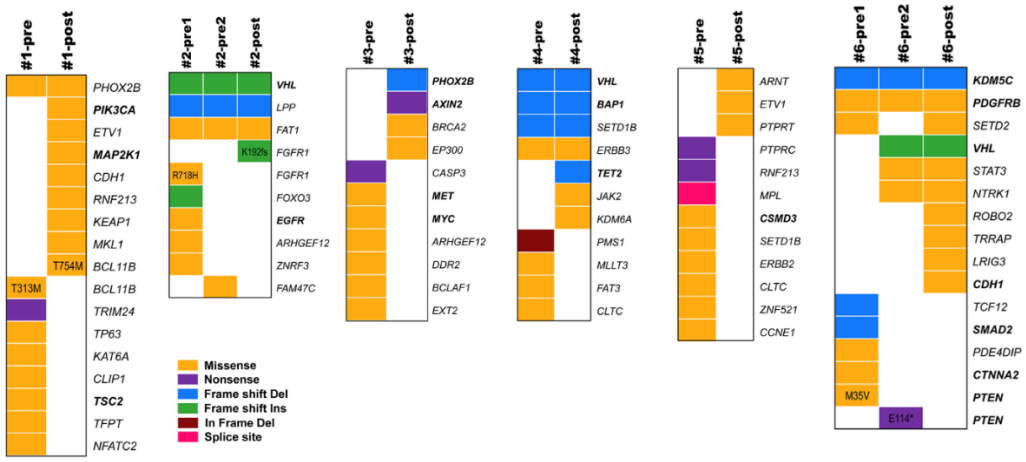

Figure 8. Somatic mutations of cancer genes detected in pre-treatment and post-treatment samples of patients showing acquired resistance.

Variants in genes marked with bold font mean oncogenic variants inferred from COSMIC, ClinVar, and OncoKB.

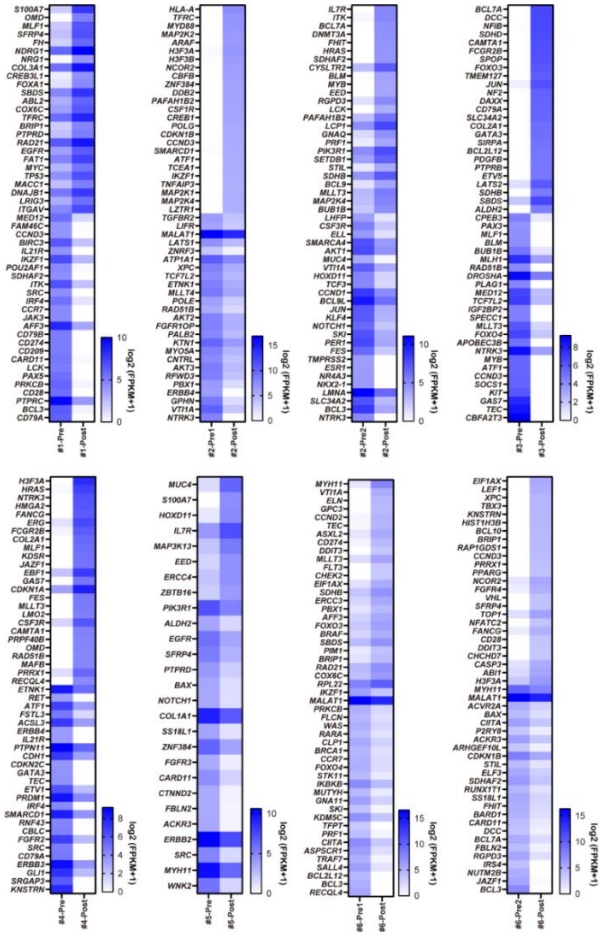

Figure 9. Heatmap of 50 top genes with average fragments per kilobase million (FPKM) of two samples ≥ 5 and log2 (fold change of FPKM) ≥ 2 as differentially expressed genes between pre-treatment and post-treatment sample.

In each patient, upregulated genes and downregulated genes in post-treatment samples are located at upper part and lower part of the heatmap bar, respectively.

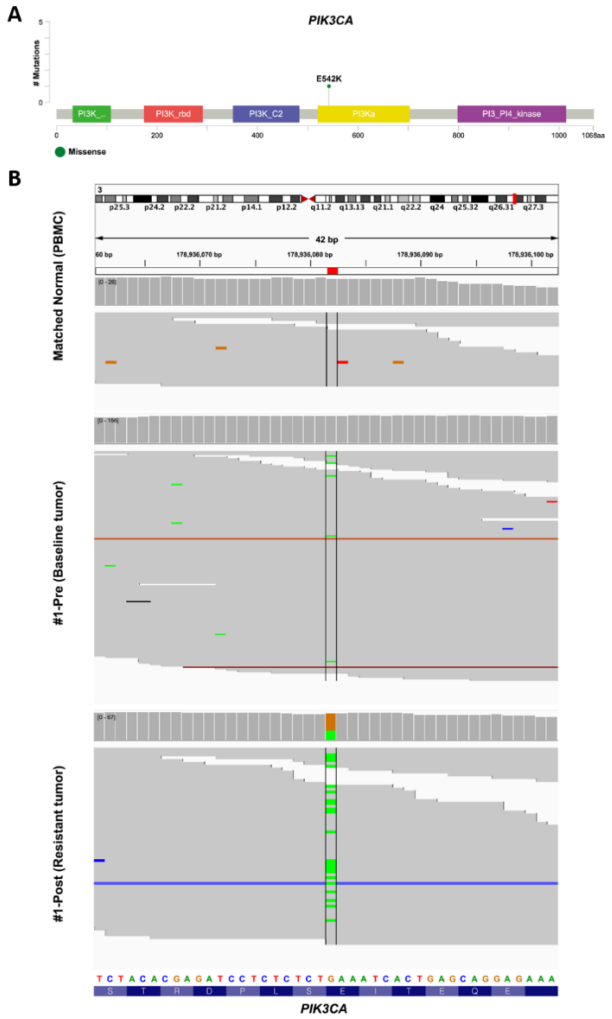

Figure 10. Acquired loss-of-function mutation in *PIK3CA* gene at the time of resistance. (A) Lollipop plot of *PIK3CA* E542K mutation located in the helical domain. (B) Integrative Genomics Viewer plots showing that the *PIK3CA* E542K missense mutation is found at the resistance.

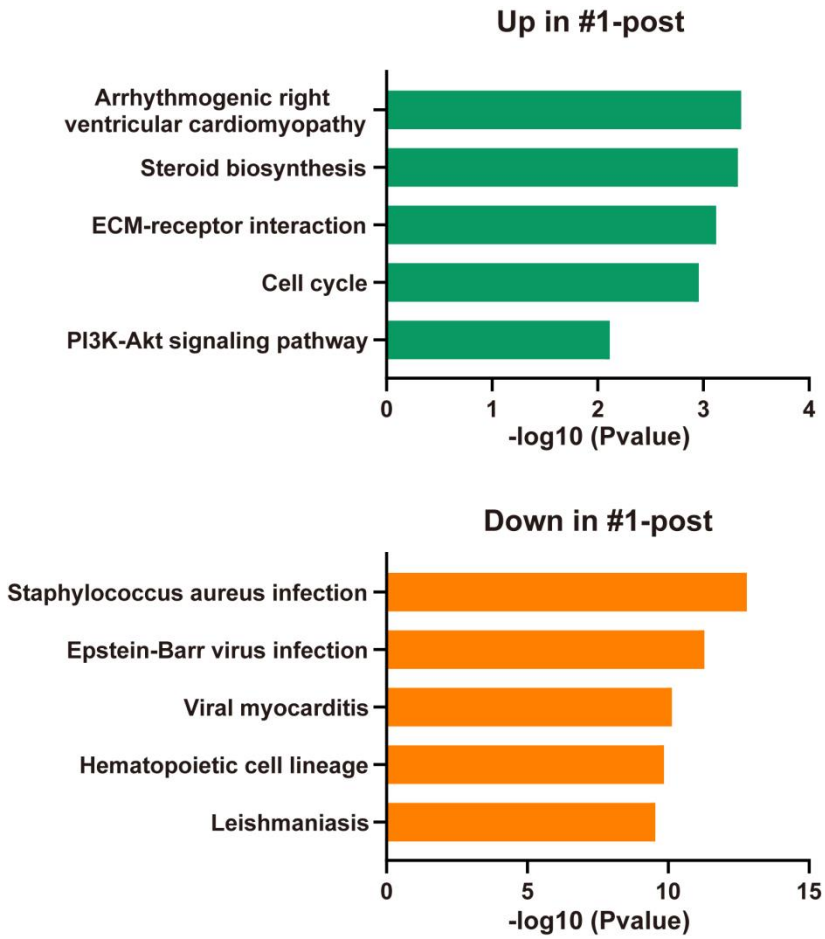

Figure 11. The pathway enrichment analysis result showing that PI3K-Akt signaling pathway was enriched in post-treatment sample of patient #1.

3.2.3.2. Activation of Wnt/β-catenin pathway

Patient #3 showed a frameshift deletion mutation (A13Pfs*35) in gene encoding paired like homeobox 2B (*PHOX2B*) and a stopgain mutation (R656*) in gene encoding *AXIN2*, which may be both likely oncogenic mutations. The Axin-related protein, Axin2, presumably plays an important role in the regulation of the stability of β-catenin in the Wnt signaling pathway (74). So, the stopgain mutation of *AXIN2* might impair the inhibition of the Wnt signaling pathway by downregulating β-catenin. Activation of Wnt/β-catenin pathway was reported previously as a mechanism of primary (75) or acquired resistance (69) to ICI. However, in pathway analysis, Wnt/β-catenin pathway was not considerably changed between pre-treatment and resistance samples of patient #3 (**Figure 12**).

3.2.3.3. Loss of *TET2*

Patient #4 showed a frameshift deletion (S424Afs*3) in gene encoding tet methylcytosine dioxygenase 2 (*TET2),* which was likely oncogenic. Loss of *TET2* was reported to be associated with decreased cancer immunity and efficacy of cancer immunotherapy (76). However, mRNA expression of TET2 was not changed in patient #4 (**Figure 9**), which implies that the frameshift deletion of TET2 may not be associated with acquired resistance.

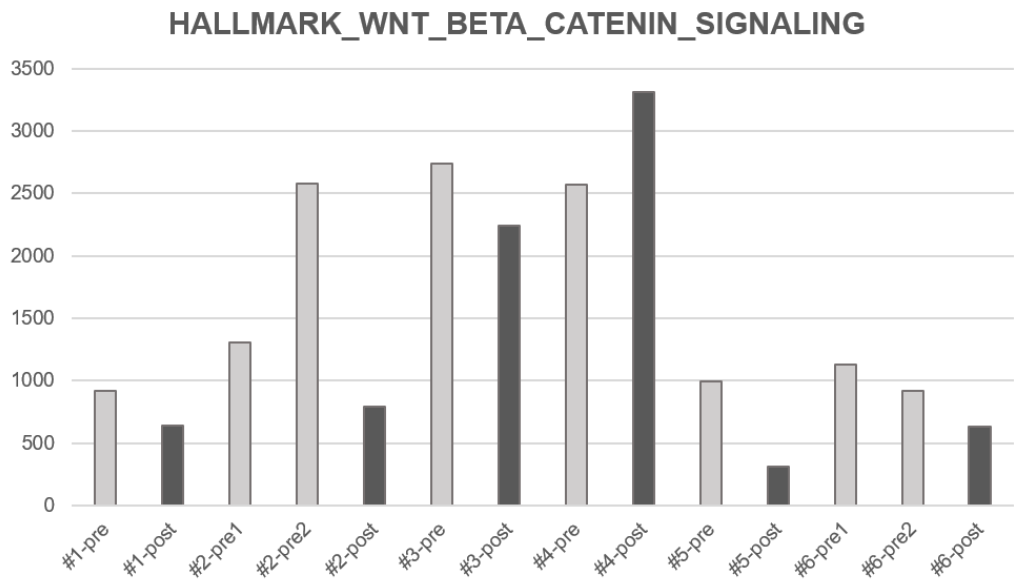

Figure 12. Wnt/β-catenin signaling pathway enrichment from Hallmark pathway database in pre-treatment and post-treatment samples.

3.2.4. PD-L1 expression on tumor cell

PD-L1 expression on tumor cell is known as a predictive biomarker for response to ICI in non-small cell lung cancer, melanoma, *etc* (77). However, predictive role of PD-L1 remains controversial in RCC and HNSCC (12, 78), while UCC patients with high PD-L1 expression on tumor cell have better treatment outcomes (79). Changes of tumor PD-L1 expression after acquisition of resistance are also inconsistent between previously reported data (29, 80, 81).

In this study, by multiplex IHC, patient #1, #3, #5, and #6 had positive PD-L1 expression on tumor cell at baseline (**Figure 13**). Tumor PD-L1 expression in pre-treatment samples of patient #2 and patient #4 was scarce. Tumor PD-L1 in patient #1 and #3 markedly decreased at the time of AR compared to the baseline, while tumor PD-L1 in patient #5 increased 3.5-fold. In patient #2 and #4, PD-L1 on tumor cells was still remained negative.

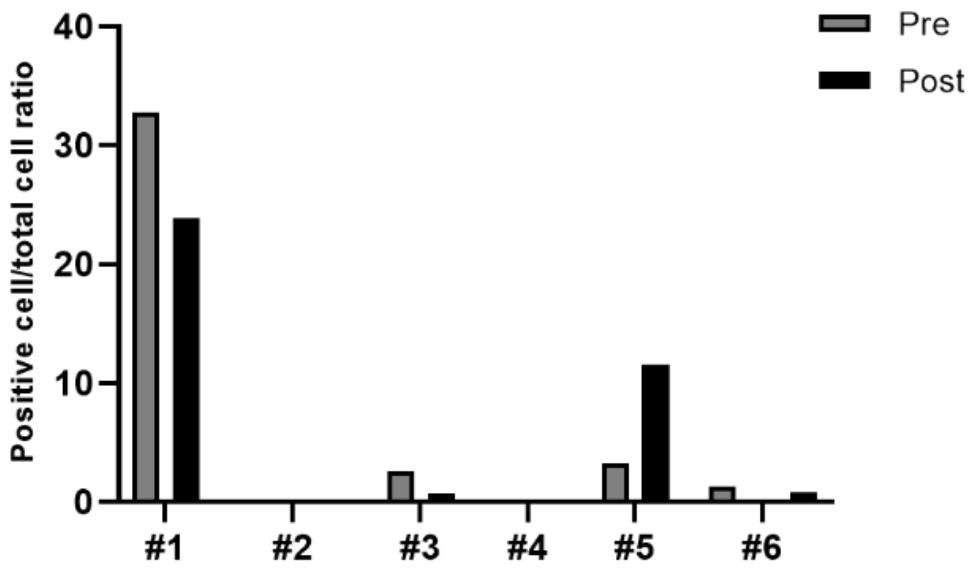

Figure 13. **The ratio of PD-L1 positive cell per total cell on CK-positive cells by multiplex immunohistochemistry.**

3.2.5. Interferon-γ associated features

To evaluate whether defective IFN-γ-related signaling, which is previously known as resistance mechanism, exists in the cohort, I explored the mutations and expression of genes which are known to be associated with the IFN-γ pathway (**Figure 14**). Except for a few missense mutations detected in post-treatment samples of patient #1, #4, and #5, no mutations conferring defects in the IFN-γ pathway were detected. No significant trend in changes in the IFN-γ-related gene expression in each gene was found, while 6-gene IFN-γ signature and IFN-γ pathway enrichment scores seemed to decrease after acquisition of resistance in patient #1 (**Figure 15**). In summary, I did not find any clear evidence of a defect in the IFN-γ pathway in our cohort.

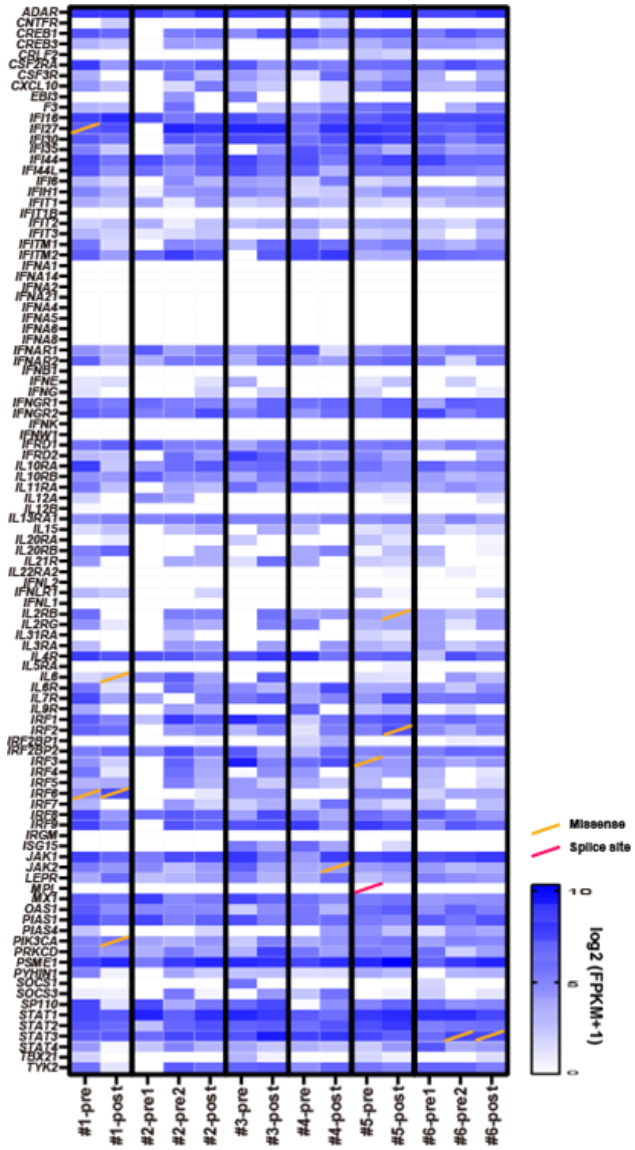

Figure 14. Expression and mutation profiles of interferon-γ pathway-associated genes.

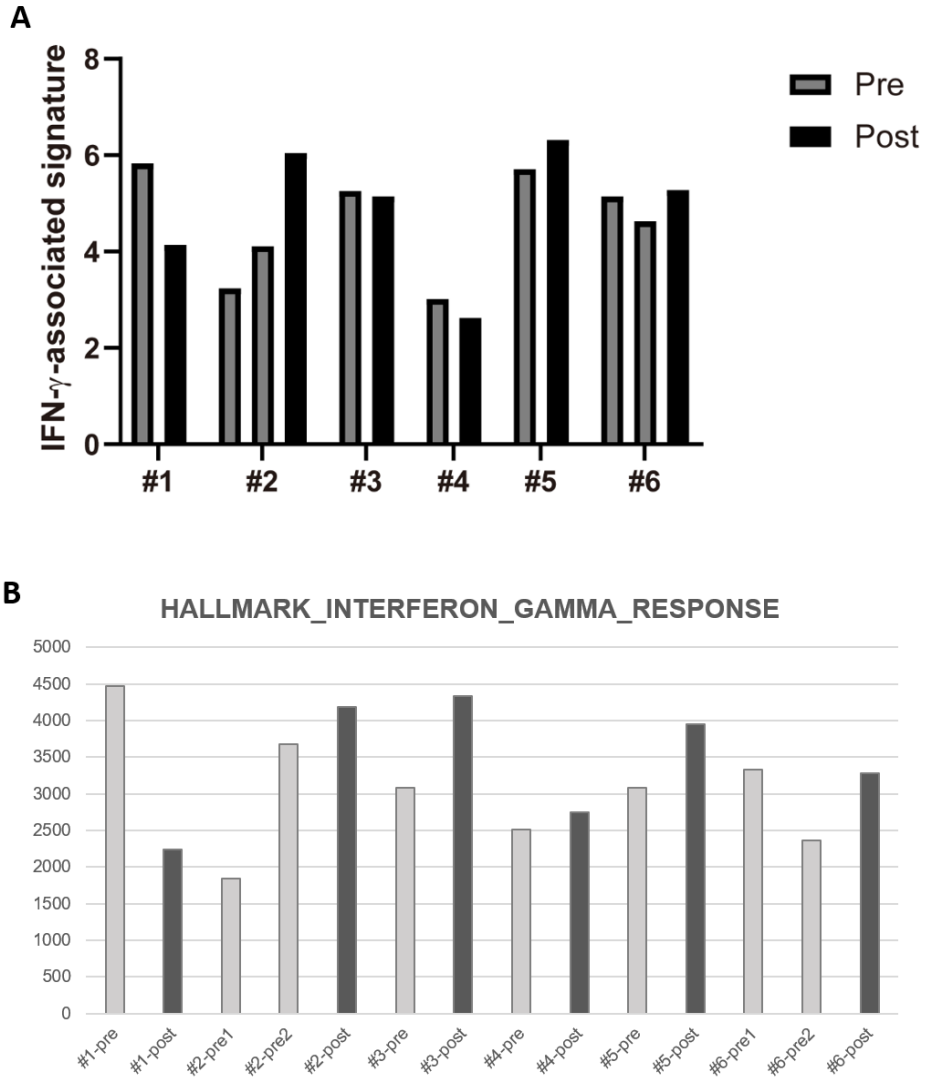

Figure 15. Interferon-γ-associated features in RNA sequencing. (A) Interferon-γ-associated signature. (B) interferon-γ pathway enrichment from Hallmark pathway database.

3.2.6. Antigen presentation machinery

To identify impaired immuno-recognition due to defective antigen presentation, I analyzed the expression status of HLA class I in CK-positive cells. None of the samples demonstrated the loss of HLA class I by multiplex IHC in post-treatment samples compared to pre-treatment samples (**Figure 16**). Moreover, the expression of antigen processing machinery-associated genes including *HLA-A, HLA-B, HLA-C,* beta-2-microglobulin (*B2M*), transporter 1 ATP binding cassette subfamily B member (*TAP1*), transporter 2 ATP binding cassette subfamily B member (*TAP2*), and TAP binding protein (*TAPBP*) was not significantly altered during ICI treatment (**Figure 17**). The WES data did not reveal any mutation related to antigen presenting machinery except for a nonsense mutation in nuclear transcription factor Y subunit gamma (*NFYC*).

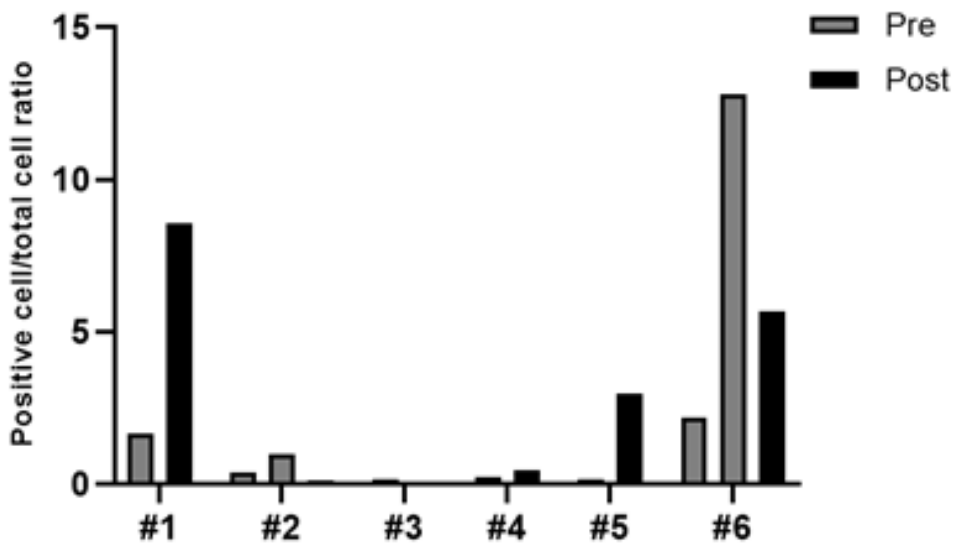

Figure 16. The ratio of HLA class I positive cell per total cell on CK-positive cells by multiplex immunohistochemistry.

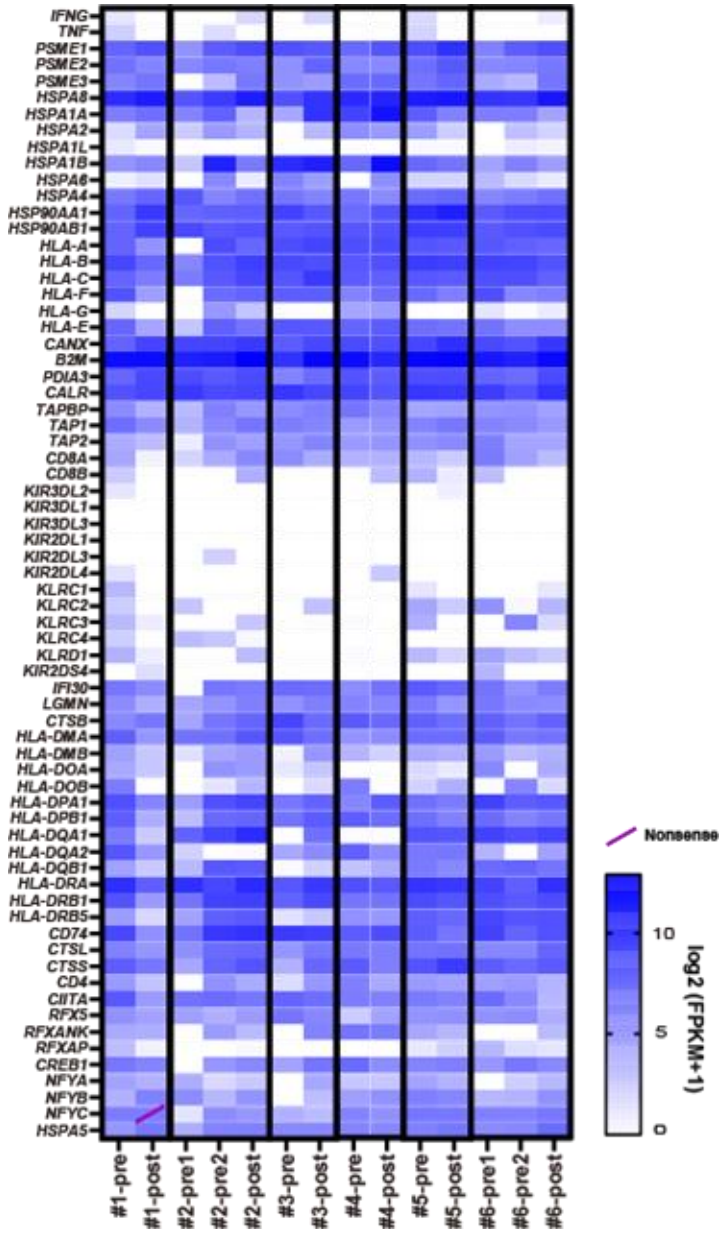

Figure 17. Expression and mutation profiles of antigen presentation machinery-associated genes.

3.3. Tumor-extrinsic: from the perspective of immune system

Genetic, transcriptomic, and pathologic changes within immune system are classified into two categories – local immunity and systemic immunity.

3.3.1. Local immunity

3.3.1.1. Tumor infiltrating lymphocytes

Tumor infiltrating lymphocytes (TIL) are the most well-known biomarker that is associated with response to ICI (17). High level of CD8-positive TILs, which features immune-inflamed tumor, is associated with better response to ICI in non-small cell lung cancer and melanoma patients (82, 83). At baseline, the amount of CD8-positive TILs varied between samples. Patient #2, #3 and #4 showed minimal CD8-positive TILs in pre-treatment samples, whereas patient #1 showed high CD8-positive TILs in pre-treatment sample (**Figure 18**). At the time of acquired resistance, multiplex IHC revealed that TILs, especially positive for CD8, were markedly decreased in patient #1 and increased in patient #2. These results were consistently shown in the RNA-seq data (**Figure 19**). The proportion of CD3, CD4, and CD8-positive cells were all increased in post-treatment samples compared to pre-treatment samples in patient #3. However, in other patient (#4, #5, and #6) the direction of the changes of TILs varied.

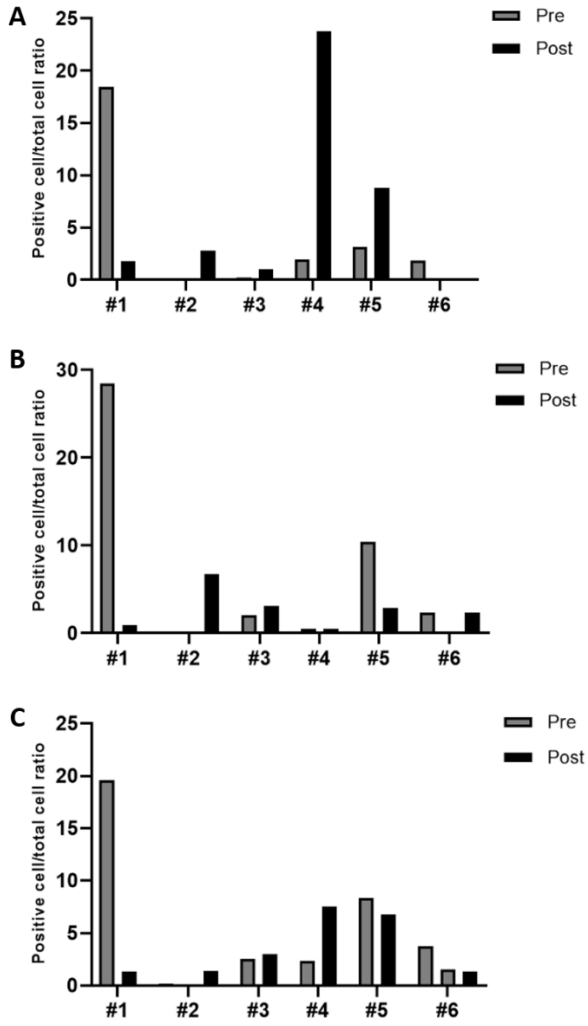

Figure 18. Pathologic evaluation of tumor-infiltrating lymphocytes by multiplex immunohistochemistry. The ratios of (A) CD3-positive cell, (B) CD8-positive cell, and (C) CD4-positive cell per total cell on CK-negative, lymphocyte-size-matched cells by multiplex immunohistochemistry are shown.

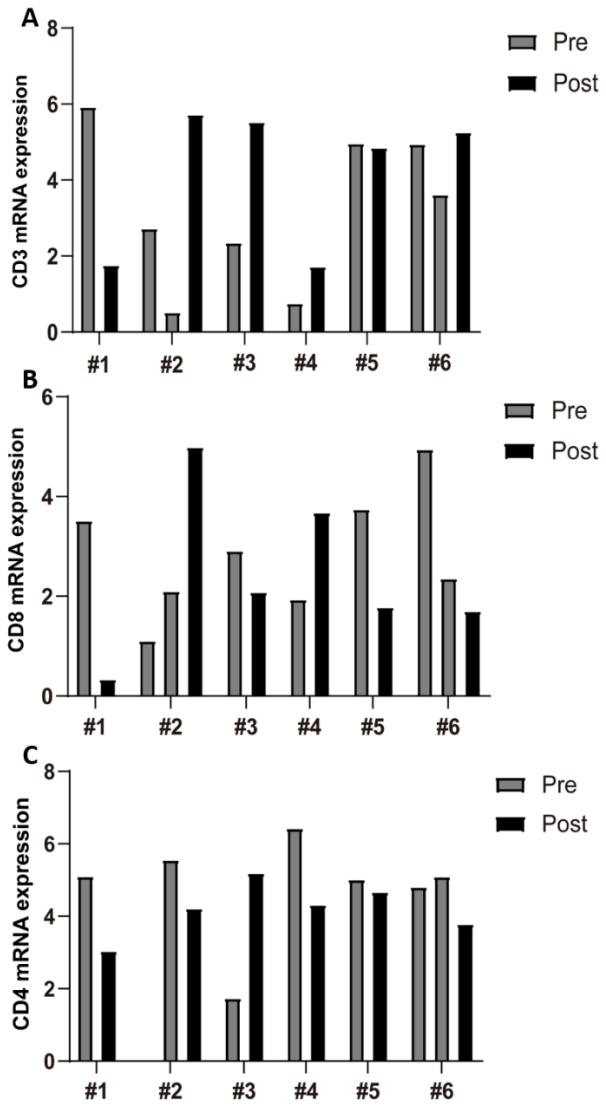

Figure 19. Transcriptomic evaluation of tumor-infiltrating lymphocytes. The mRNA expression levels of (A) CD3, (B) CD8 and (C) CD4 in pre-treatment and post-treatment samples by RNA sequencing are shown.

3.3.1.2. Immune checkpoints and immune-activation gene expression

Immune checkpoints are crucial molecules that differentially express on immune cell surface and negatively regulate immune response (84). The major checkpoints are located on T cell, which may result in immune escape by T cell exhaustion (85). I examined the expression of the major three checkpoints which are associated with T cell exhaustion – PD-1, LAG3 and TIM3 by multiplex IHC. In addition, the expressions of 22 genes encoding immune checkpoint molecules were also investigated by RNA sequencing. In patient #2, while at baseline PD-1, LAG3 and TIM3 were hardly expressed, those were all elevated in post-treatment sample (**Figure 20 and Figure 21**). Consistent with multiplex IHC data, these were similarly seen in RNA-seq data (**Figure 22**). *CTLA-4* also increased in post-treatment sample of patient #2. On the other hand, immune checkpoints including PD-1, LAG3, and TIM3 were all decreased in the post-treatment samples of patient #1 (**Figure 21 and Figure 22**). In patient #3, all the immune checkpoints were minimally expressed and not changed much. Patient #4 exhibited the decrease of PD-1 only, neither LAG3 nor TIM3. *VISTA*, which is encoded by the *C10orf54* gene, has been reported to be associated with negative immune response (86). However, none of the patients except for patient #4 had increased *VISTA* expression in post-treatment (**Figure 22**).

mRNA expression of immune activation markers were investigated by RNA sequencing. The decreasing trend of immune activation markers such as *IFNG*,

perforin 1 (*PRF1*), granzyme A (*GZMA*), granzyme A (*GZMB*), cystatin F (*CST7*), and natural killer cell granule protein 7 (*NKG7*) was observed in the post-treatment sample of patient #1. On the other hand, the elevated expressions of immune activation markers and cytolytic activity were observed at the time of acquired resistance in patient #2 (**Figure 22 and Figure 23**).

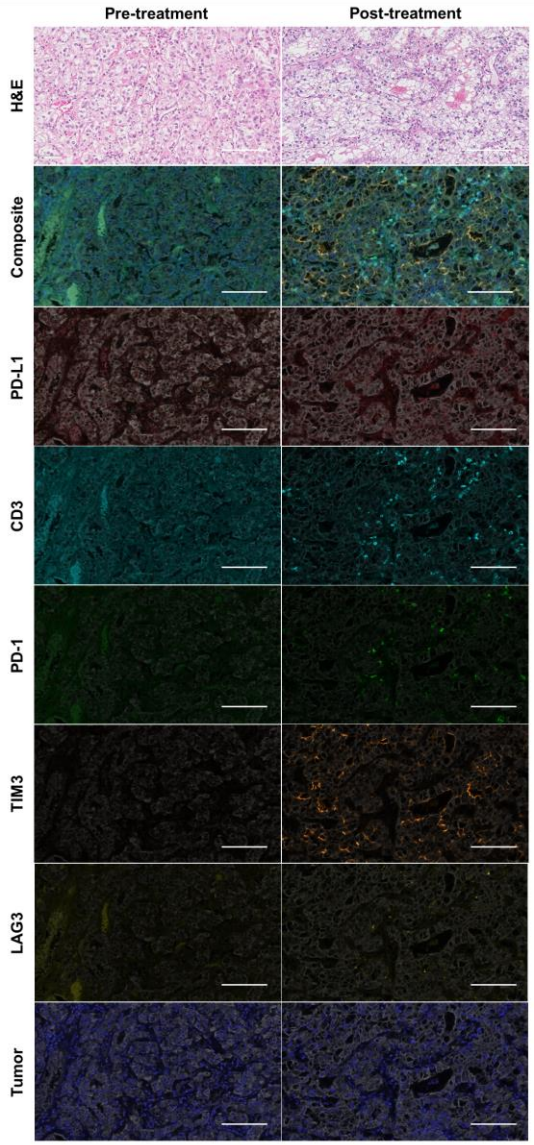

Figure 20. H&E, PD-L1, CD3, PD-1, LAG3, and TIM3 immunohistochemical staining of the tumors before and after ICIs in patient #2. (scale bar, 100um)

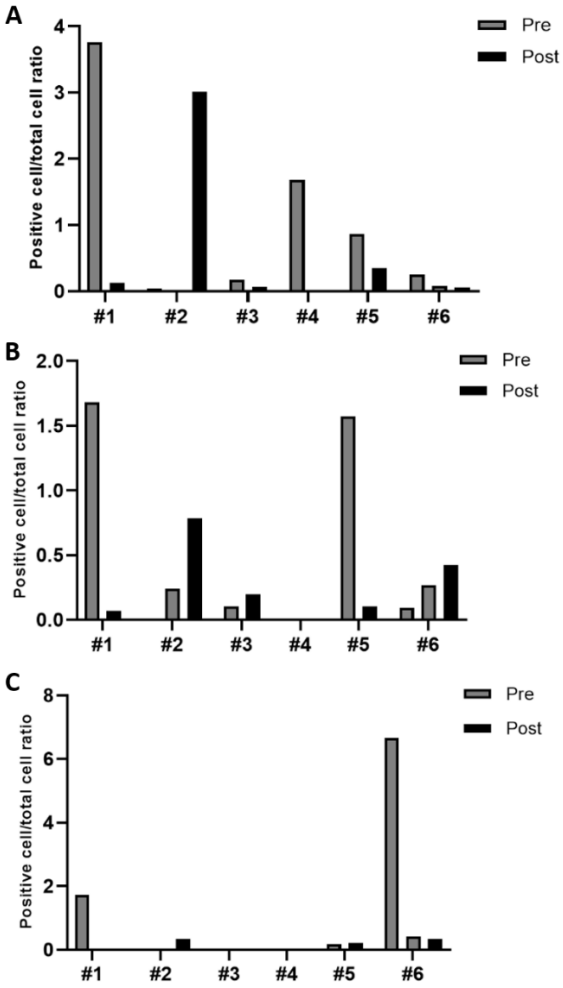

Figure 21. Pathologic evaluation of three immune checkpoints by multiplex immunohistochemistry. The ratios of (A) PD-1-positive cell, (B) LAG3-positive cell, and (C) TIM3-positive cell per total cell on CK-negative, lymphocyte-size-matched cells by multiplex immunohistochemistry are shown.

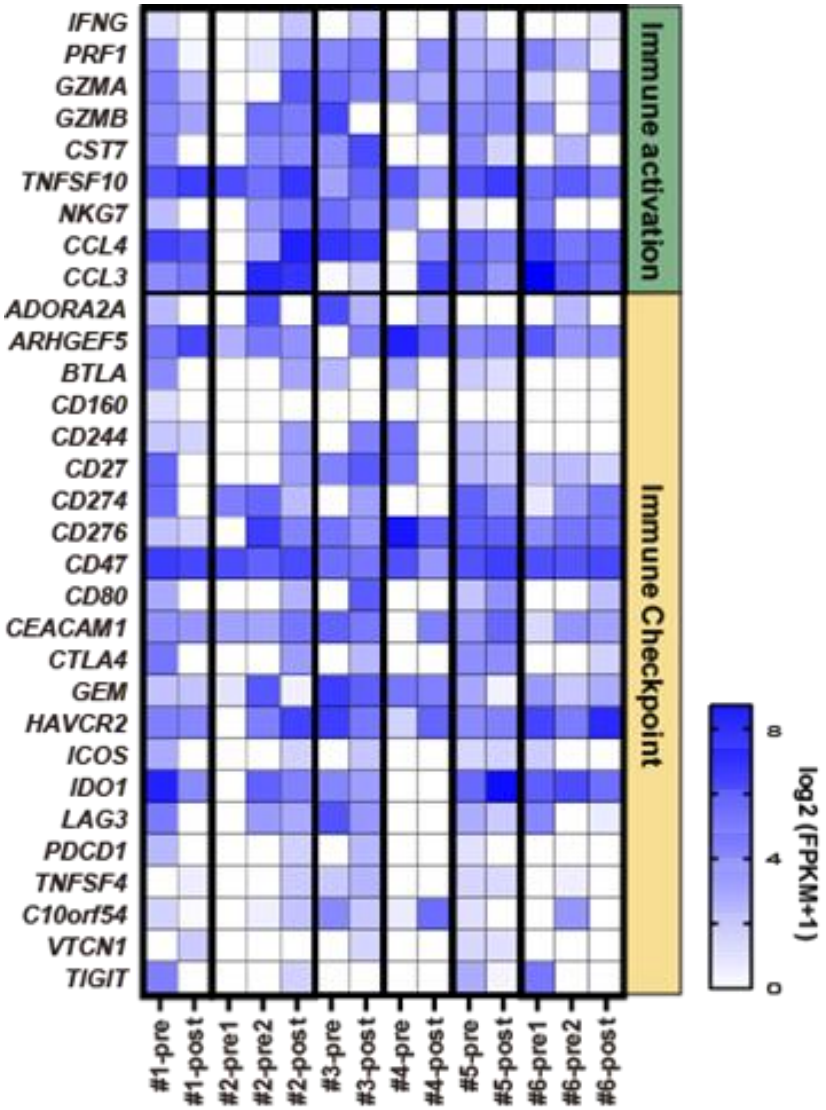

Figure 22. Heatmap comparison of the expression of genes related to immune activation and immune suppression (immune checkpoint) between pre-treatment and post-treatment samples by RNA sequencing.

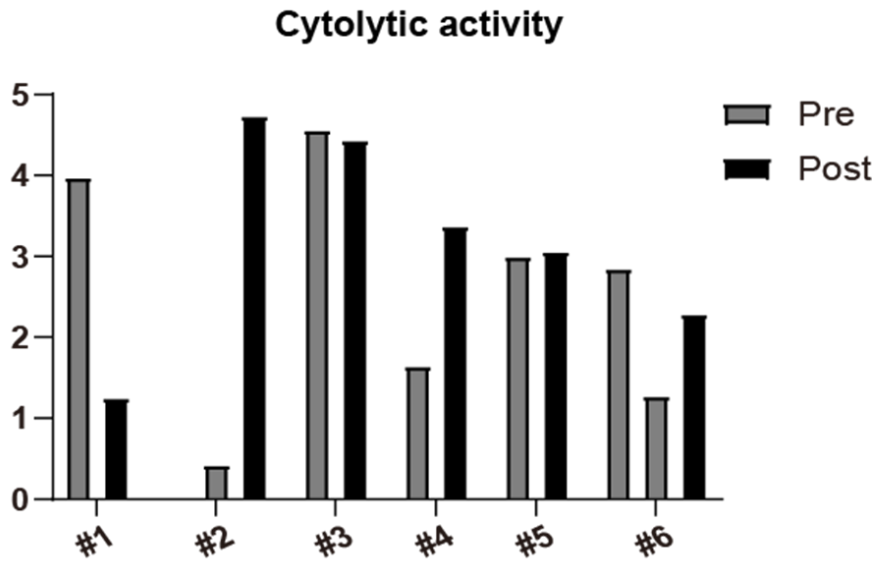

Figure 23. Cytolytic activity by RNA sequencing.

3.3.1.3. Immune cells within tumor microenvironment

The components of the tumor microenvironment and their changes before and after ICI treatment were evaluated using CIBERSORT (**Figure 24**).

Although regulatory T cells play a role in downregulation of immune responses (65, 87), I did not observe their presence in the samples. The difference in the abundance of macrophages between pre-treatment and post-treatment samples was observed in some patients. The proportions of M1 and M2 macrophages both increased in the post-treatment sample of patient #1. On the other hand, the proportion of M2 macrophage was elevated in post-treatment sample of patient #3. I also performed multiplex IHC for CD86 (representative of M1 macrophage) and CD163 (representative of M2 macrophage) (**Figure 25)**. From the multiplex IHC analysis, the ratio of CD86-positive cell and CD163-positive cell per total cell both decreased in the post-treatment sample of patient #1, which was inconsistent with CIBERSORT analysis of RNA-seq. The change of CD163-positive cell per total cell between pre-treatment and post-treatment samples in patient #3 was also inconsistent with the result from CIBERSORT analysis. I observed that M1 and M2 macrophage both increased in the post-treatment sample of patient #5, whereas M2 macrophage only increased in the post-treatment sample of patient #2.

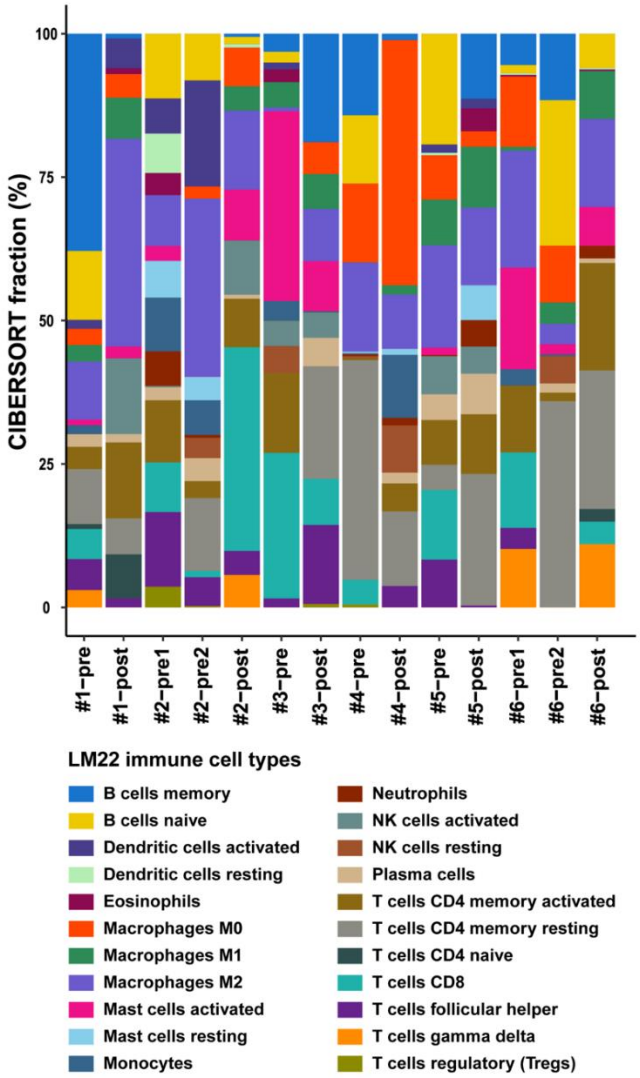

Figure 24. Comparison of the fraction of immune cell population estimated by CIBERSORT between pre-treatment and post-treatment samples.

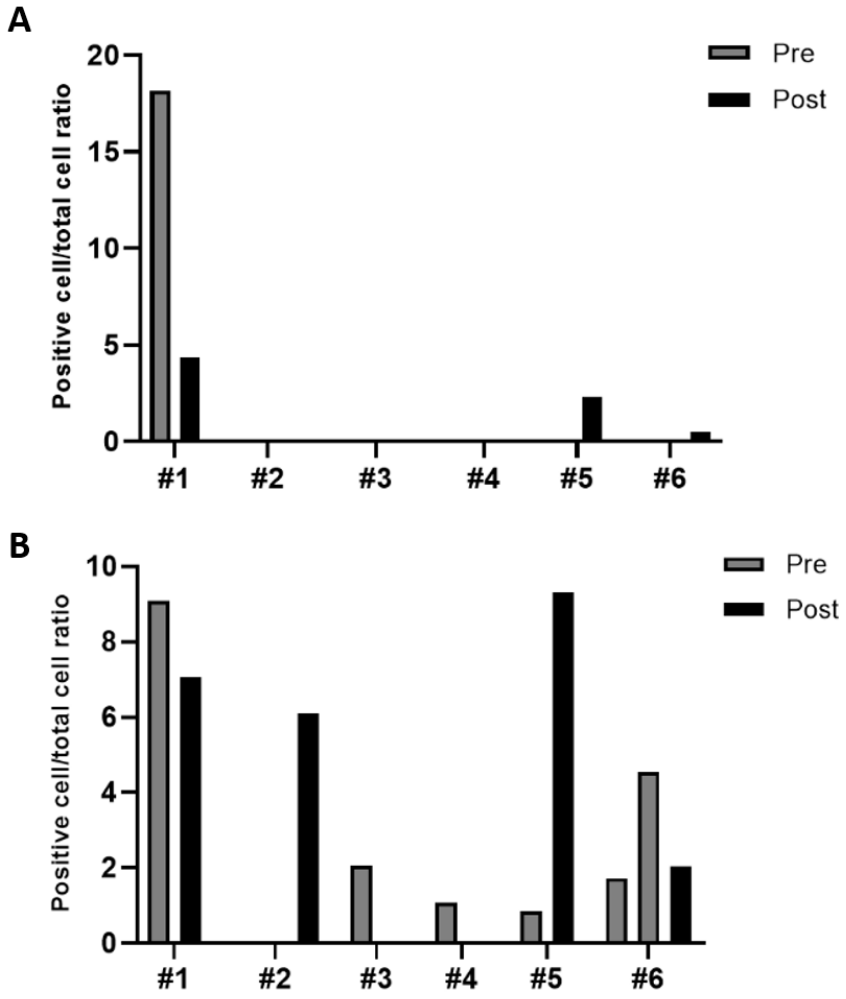

Figure 25. **Pathologic evaluation of macrophages by multiplex immunohistochemistry.** The ratio of (A) CD86-positive cell and (B) CD163-positive cell per total cell on CK-negative, macrophage-size-matched cells by multiplex immunohistochemistry are shown.

3.3.2. Systemic immunity

3.3.2.1. Neutrophil-to-lymphocyte ratio

The neutrophil-to-lymphocyte ratio (NLR) is a marker of systemic inflammation. It was shown to be associated with treatment outcomes in patients who treated with ICIs (88, 89). Although there are debates about the optimal cut-off value of high NLR (90), NLR > 5 was considered to be high in ICI studies (91-93). Changes in NLR after acquisition of resistance to ICIs remain unclear yet. In this cohort, trends of NLR varied between patients (**Figure 26**). During ICI treatment, NLR remained under 5 in two patients (patient #2 and #5). In patient #1 and #3, high NLR at the initiation of ICI decreased during the treatment, then elevated again before progression. Similarly, patient #6 also showed elevated NLR at the time of progression. In patient #4, NLR was fluctuated during the treatment.

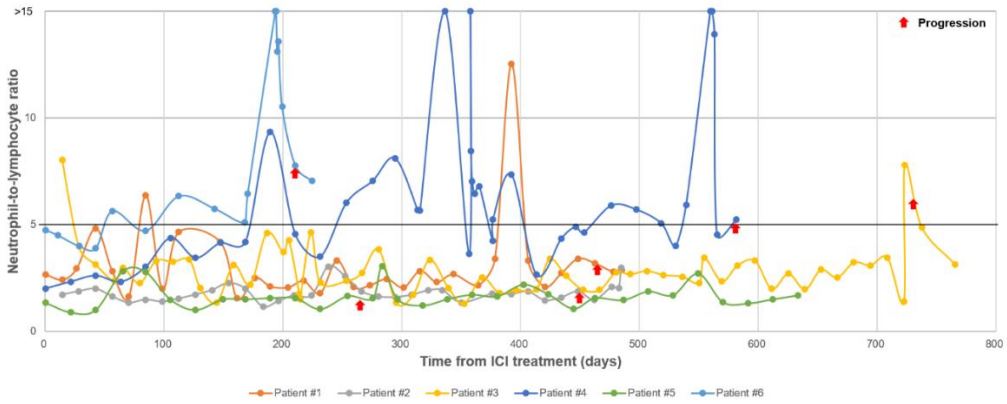

Figure 26. Changes in neutrophil-to-lymphocyte ratio in six patients during ICI treatment.

Red arrow indicates the time of progression.

3.3.2.2. Serum lactate dehydrogenase

Elevated pretreatment serum lactate dehydrogenase (LDH) was reported to be associated with poor response to ICIs in cancer patients (94). Change of LDH during acquired resistance has not been elucidated yet. In this cohort, the LDH level was not elevated (< 250) in all the patients from pretreatment to progression (**Figure 27**).

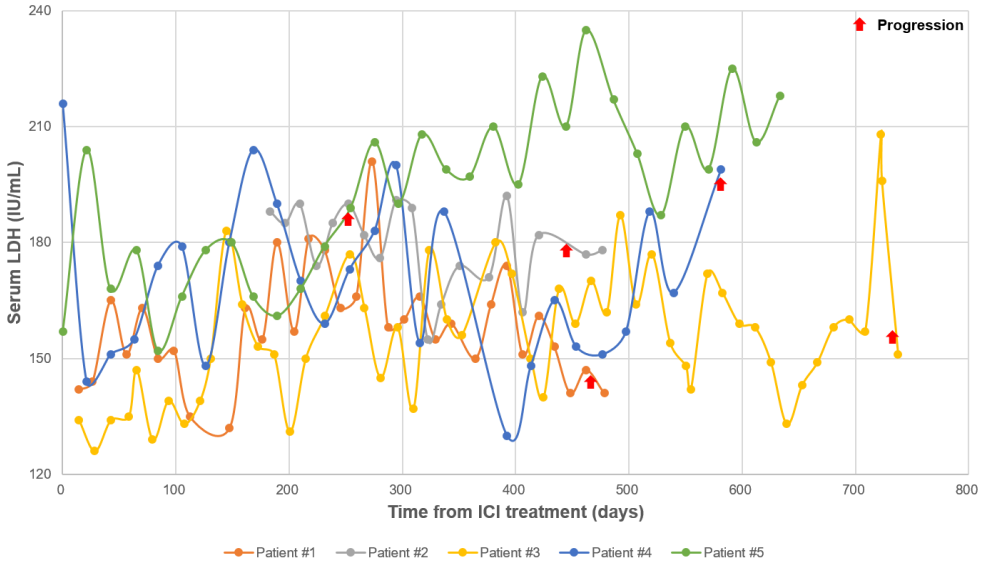

Figure 27. Changes in serum lactate dehydrogenase (LDH) in five patients during ICI treatment. Red arrow indicates the time of progression.

4. DISCUSSION

Although the number of research focusing on the efficacy of immunotherapy rapidly increases, little has been elucidated about genetic, transcriptional and pathologic changes after acquisition of resistance in patients who are treated with ICIs so far (5, 19). The defect of antigen presenting machinery (29, 30, 95), loss of neo-antigen (32), or loss-of-function mutation in IFN-γ signaling pathway (29, 96) has been reported to result in acquired resistance to ICIs in previous studies. However, no specific mechanism is identified in many cases and the true landscape of acquired resistance to ICIs remains still unveiled (18). In this study, the changes related to previously known mechanism were partly seen in some cases, and in others the changes supporting different possible mechanism of resistance were found.

I classified the genetic, transcriptional and pathologic changes related to acquired resistance to ICIs, which have been reported in previous studies and found in this study, into two categories: tumor-intrinsic (tumor side) and tumor-extrinsic (immune side) (**Figure 28**). In this study, one patient (patient #1) showed genetic changes in tumor-intrinsic components, and two patients (patient #3 and #4) had possible genetic changes in tumor-intrinsic components which may not be associated with acquired resistance. Two patients (patient #2 and #5) mainly showed the changes in local immunity, without clear changes in tumor-intrinsic components.

No definite changes were noted in one patient (patient #6).

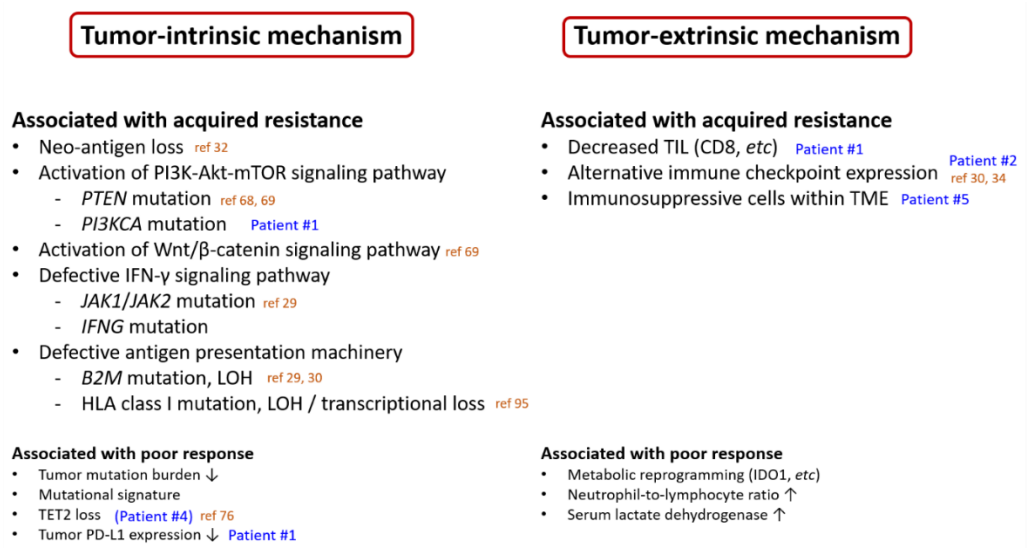

Figure 28. Summary of tumor-intrinsic and tumor-extrinsic mechanisms of acquired resistance

Abbreviation: LOH, loss-of-heterozygosity; TME, tumor microenvironment;

4.1. Changes in tumor-intrinsic components

Changes in tumor-intrinsic components during ICI treatment comprise either changes in oncogenic signaling pathways that affect the immunity or changes directly related to immune regulation. Genetic alterations in several key oncogenic and tumor suppressor pathways are important not only for playing a role in tumor cells and developing cancer, but also for modulating the regulation of immune checkpoints and affecting immune escape (97). The PI3K-Akt-mTOR signaling pathway is a commonly known oncogenic signaling pathway, which plays a crucial role in cell growth, proliferation, and metabolism (98), and is frequently activated in aberrant ways in many cancer types (66, 98). This pathway is also associated with the regulation of immune checkpoints and sensitivity to ICIs (97). Activation of the PI3K-Akt-mTOR pathway was related to increased expression of PD-L1 in glioblastoma (99), breast and prostate cancer (100), and inhibition of the pathway had synergistic effect with anti-PD-1 inhibitor in syngeneic and genetically engineered mouse models of lung cancer (101). Loss of *PTEN*, which can activate PI3K-Akt-mTOR pathway, was reported to decrease T-cell infiltration and upregulate immunosuppressive cytokines in preclinical model of melanoma (70). *PI3KCA* mutation, as another genetic aberration in PI3K-Akt-mTOR pathway, was also associated with less immune gene expression in muscle-invasive bladder cancer patients (102). Although loss of *PTEN* has been considered as a change related to acquired resistance to ICIs in a leiomyosarcoma patient (68) and a melanoma patient (69), to my knowledge, it is the first that acquired *PIK3CA*

mutation was found in the patient who treated with ICI and showed acquired resistance. I observed that significant decreases of the immune infiltrates such as TILs and several immune activation markers were found in post-treatment sample of patient #1 and that PI3K-Akt pathway was enriched in post-treatment sample. It is consistent with the result from previous study in bladder cancer patients (102) that tumor-immune infiltrates were decreased in *PI3KCA*-mutated population. Inhibition of PI3K-Akt-mTOR signaling pathway using different PI3K inhibitors was effective for promoting tumor regression, restoring immune infiltrates, and enhancing response to ICIs, as reported in several studies (102-104). I propose that PI3K inhibition in addition to ICI treatment would be beneficial to overcome acquired resistance in patient #1.

Another interesting finding from patient #1 is that the tumor clone with *PIK3CA* E542K mutation expanded significantly during acquisition of resistance in a HPV-positive HNSCC patient which has predominant APOBEC feature before ICI treatment. APOBEC3 appear to play a role in HPV-associated carcinogenesis by generating somatic mutations on the basis of viral oncoprotein (E6 and E7) expression (105). In addition, APOBEC-signature, which is characterized by C>T transitions and C>G transversions at TpC dinucleotides (65, 71, 106) is also widely found in HNSCC, especially for HPV-positive HNSCC due to reduced exposure to exogenous carcinogen such as smoking (107). The presence of APOBEC-signature was associated with high TMB (64, 108), which can explain better response to ICI treatment (109, 110). So I suppose that high level of TMB and its increase at post-

treatment may be related to predominant APOBEC-signature and initial response in patient #1. Among mutations of the PI3K pathway, which are frequently found in HNSCC patients (111, 112), E542K (c.1624G > A) mutation in the helical domain of the *PIK3CA* gene can be caused by APOBEC-mediated TCW mutation, as reported in a study of HPV-positive HNSCC tumors from The Cancer Genome Atlas HNSCC cohort (107). The observation that *PIK3CA* DNA is deaminated by APOBEC3B in vitro can explain that (107). The hypothesis I propose is that the newly detected E542K mutation in *PIK3CA* helical domain may result from APOBEC activity and lead to immune escape at the time of acquired resistance by decreasing the immune infiltrates (**Figure 29**).

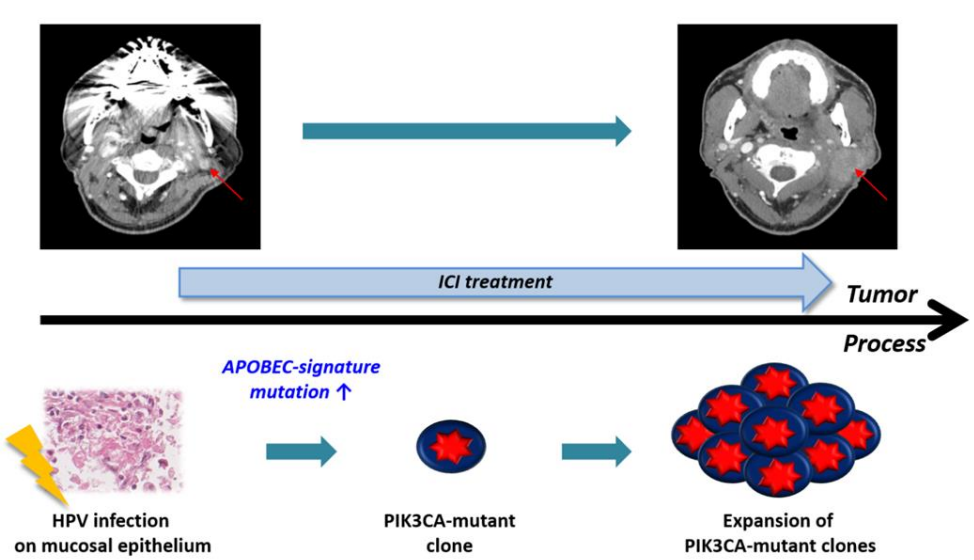

Figure 29. Hypothetical diagram indicating the development of *PIK3CA*-mutant clones mediated by *APOBEC*-signature in HPV-infected head and neck squamous cell carcinoma patient.

Wnt/β-catenin signaling pathway is also one of oncogenic signaling pathway that can be associated with resistance to ICIs (97, 113). Activation of Wnt/β-catenin signaling pathway was also reported to be associated with acquired resistance to immunotherapy in a melanoma patient (69). The aberrant activation of the Wnt/β-catenin signaling pathway results in T cell infiltration and dendritic cell inhibition (114), so it may impair the therapeutic activity of ICIs. A stop-gain mutation in gene encoding *AXIN2*, which was found in patient #3, may activate Wnt/β-catenin signaling pathway by disruption of negative regulation feedback. However, in this patient, Wnt/β-catenin signaling pathway was not enriched in post-treatment sample, so this would not actually contribute to acquired resistance. Similarly, loss of *TET2* was found in patient #4, which could be associated with immune evasion from anti-PD-1 treatment (76). In a preclinical study of melanoma and colon cancer, *TET2* control chemokine, PD-L1 expression, TIL infiltration by mediating the IFN-γ-JAK-STAT signaling pathway. *TET2* deletion reduced chemokine expression and TILs, leading the tumor to immune escape. However, these features were not evident in the patient #4. It is important to differentiate descriptive findings versus mechanisms of acquired resistance (18). Further exploration about interaction of changes in tumor-intrinsic and tumor-extrinsic components in patients such as patient #3 and #4 is needed.

The two most widely studied changes in tumor-intrinsic components related to immune regulation are defective antigen presentation and defects in IFN-γ signaling. Prior studies in patients who treated with ICI and showed acquired

resistance demonstrated that disruption of antigen presentation could play a key role in immune evasion of tumor even if the level of cytotoxic CD8-positive TIL remains elevated (29-31, 95). However, this study finding that no events were detected in genes related to antigen presentation in the cohort samples suggests that immuno-recognition can be intact at the time of resistance and different mechanisms may work to induce acquired resistance. Moreover, JAK-STAT signaling and IFN-γ pathway are associated with maintenance of cell senescence to keep remnant tumor cells dormant (115), defects in those pathways could have caused acquired resistance in patients treated with ICI. However, mutations in *JAK1* or *JAK2* that can lead to decreased sensitivity to IFN-γ were also not detected in this cohort samples.

4.2. Changes in tumor-extrinsic components

One of the key changes in tumor-extrinsic components (immune side) is upregulation of alternative immune checkpoints (85). I found that the expression level of alternative immune checkpoints such as *TIM3*, *LAG3*, or *CTLA4* elevated during acquisition of resistance against ICI treatment in patient #2. It is consistent with the result from previous studies that upregulation of *TIM3* on TIL was observed in the mouse model, melanoma and non-small cell lung cancer patients showing acquired resistance to ICI treatment (34, 116, 117). In a preclinical study of HNSCC tumors, adaptive resistance to anti-PD-1 inhibitor was led by *TIM3* upregulation in a PI3K-Akt-dependent manner (118). In addition, mRNA expression

level of *LAG3* was elevated in resistant tissues compared to pre-immunotherapy tissues in non-small cell lung cancer patients (30). Immunosuppressive alternative checkpoints such as *TIM3* or *LAG3* play a compensatory role limiting tumor-reactive T-cell function and would make tumors escape from therapeutic blockade of PD-1 / PD-L1 axis (85). Although TILs, especially positive for CD8, increased at the time of resistance, immunosuppressive signals around tumor microenvironment may interact with TILs and impair their function to kill tumor cells (5, 119). In patient #2, no significant mutations or copy number alterations were detected, so these transcriptional changes of alternative immune checkpoints may be associated with acquired resistance. Sequential treatment for inhibiting these immunosuppressive checkpoints might be a strategy for overcoming acquired resistance (34, 120).

In patient #5, increased proportion of M2 macrophage, which plays an immunosuppressive role within tumor microenvironment, was observed in post-treatment sample. M2 macrophage can enhance tumor growth, invasion and metastasis through secretion of anti-inflammatory cytokines and pro-angiogenic factors (121). Targeting for immunosuppression mediated by tumor-associated macrophage can be a potential therapeutic approach to enhance anti-tumor immune response (122). Although immunosuppressive components within tumor microenvironment including myeloid-derived suppressor cell, cancer-associated fibroblast, or regulatory T cell may contribute to immunotherapy resistance (19, 123, 124), other components of tumor microenvironment than macrophage were not

changed in this cohort patients. In patient #5, little changes in tumor-intrinsic components were observed, so in such case, evaluation of tumor-extrinsic components, especially for immune cell subpopulation, is important to explore the mechanism of resistance.

4.3. Clinical implications and limitations

Some clinical implications are drawn from this study. First, it was a hypothesis generating study investigating the changes associated with potential mechanism of acquired resistance, which can suggest further studies for confirmation and validation of the impact of those changes on acquired resistance. Although there have been several studies exploring the mechanism of acquired resistance using WES, RNA-seq, or immunohistochemistry so far, the insights for the true landscape of acquired resistance to ICIs remains still uncertain, and further data should be accumulated. This study can give an underpinning clue to expand the research area. Second, classifying the changes of parameters into tumor-side and immune-side can help systematically identify which changes are the main ones related to acquired resistance. Despite several efforts to figure out the mechanism of acquired resistance, to date, there has been relatively no therapeutic progress to reverse acquired resistance. Although multi-facet approaches are needed to explore the resistance mechanism, it is essential to target the main changes for therapeutic strategies (85). This kind of classification can aid to plan therapeutic strategies.

This study has several limitations. Firstly, the number of patients included in

this study was small due to unavailability of pre-treatment and post-treatment tissues for WES, RNA-seq, and multiplex IHC. Further prospective studies with sufficient patients who display acquired resistance are needed. Secondly, whether *PIK3CA* mutagenesis can lead to acquired resistance or is just a coincident event with tumor progression should be validated in an animal model or in another patient cohort. Lastly, mutations in tumor samples with relatively low purity might not be detected and missed as false negatives.

4.4. Conclusion

This study showed that the increases of alternative immune checkpoints seen at the time of resistance may contribute to the acquired resistance in one clear cell RCC patient. Different from this case, I found a hotspot mutation in gene encoding *PIK3CA*, which may be mediated by APOBEC-associated signature, and suggest that this mechanism can possibly contribute to the acquired resistance in another HPV-positive HNSCC patient. However, previously known mechanism of acquired resistance – defect of antigen presentation or defect of IFN-γ signaling – were not detected.

REFERENCES

1. Vaddepally RK, Kharel P, Pandey R, Garje R, Chandra AB. Review of Indications of FDA-Approved Immune Checkpoint Inhibitors per NCCN Guidelines with the Level of Evidence. Cancers (Basel). 2020;12(3).

2. Wattenberg MM, Fong L, Madan RA, Gulley JL. Immunotherapy in genitourinary malignancies. Curr Opin Urol. 2016;26(6):501-7.

3. Cohen EEW, Bell RB, Bifulco CB, Burtness B, Gillison ML, Harrington KJ, et al. The Society for Immunotherapy of Cancer consensus statement on immunotherapy for the treatment of squamous cell carcinoma of the head and neck (HNSCC). J Immunother Cancer. 2019;7(1):184.

4. Champiat S, Ileana E, Giaccone G, Besse B, Mountzios G, Eggermont A, et al. Incorporating immune-checkpoint inhibitors into systemic therapy of NSCLC. J Thorac Oncol. 2014;9(2):144-53.

5. Sharma P, Hu-Lieskovan S, Wargo JA, Ribas A. Primary, Adaptive, and Acquired Resistance to Cancer Immunotherapy. Cell. 2017;168(4):707-23.

6. Zappasodi R, Merghoub T, Wolchok JD. Emerging Concepts for Immune Checkpoint Blockade-Based Combination Therapies. Cancer Cell. 2018;33(4):581-98.

7. Gridelli C, Casaluce F. Frontline immunotherapy for NSCLC: alone or not alone? Nat Rev Clin Oncol. 2018;15(10):593-4.

8. Helmink BA, Gaudreau PO, Wargo JA. Immune Checkpoint Blockade across the Cancer Care Continuum. Immunity. 2018;48(6):1077-80.

9. Darvin P, Toor SM, Sasidharan Nair V, Elkord E. Immune checkpoint inhibitors:

recent progress and potential biomarkers. Exp Mol Med. 2018;50(12):1-11.

10. Chen JA, Ma W, Yuan J, Li T. Translational Biomarkers and Rationale Strategies to Overcome Resistance to Immune Checkpoint Inhibitors in Solid Tumors. Cancer Treat Res. 2020;180:251-79.

11. Xiao Q, Nobre A, Pineiro P, Berciano-Guerrero MA, Alba E, Cobo M, et al. Genetic and Epigenetic Biomarkers of Immune Checkpoint Blockade Response. J Clin Med. 2020;9(1).

12. Davis AA, Patel VG. The role of PD-L1 expression as a predictive biomarker: an analysis of all US Food and Drug Administration (FDA) approvals of immune checkpoint inhibitors. J Immunother Cancer. 2019;7(1):278.

13. Patel SP, Kurzrock R. PD-L1 Expression as a Predictive Biomarker in Cancer Immunotherapy. Mol Cancer Ther. 2015;14(4):847-56.

14. Kim JY, Kronbichler A, Eisenhut M, Hong SH, van der Vliet HJ, Kang J, et al. Tumor Mutational Burden and Efficacy of Immune Checkpoint Inhibitors: A Systematic Review and Meta-Analysis. Cancers (Basel). 2019;11(11).

15. Klempner SJ, Fabrizio D, Bane S, Reinhart M, Peoples T, Ali SM, et al. Tumor Mutational Burden as a Predictive Biomarker for Response to Immune Checkpoint Inhibitors: A Review of Current Evidence. Oncologist. 2020;25(1):e147-e59.

16. Hellmann MD, Ciuleanu TE, Pluzanski A, Lee JS, Otterson GA, Audigier-Valette C, et al. Nivolumab plus Ipilimumab in Lung Cancer with a High Tumor Mutational Burden. N Engl J Med. 2018;378(22):2093-104.

17. Arora S, Velichinskii R, Lesh RW, Ali U, Kubiak M, Bansal P, et al. Existing and Emerging Biomarkers for Immune Checkpoint Immunotherapy in Solid Tumors. Adv Ther. 2019;36(10):2638-78.

18. Schoenfeld AJ, Hellmann MD. Acquired Resistance to Immune Checkpoint Inhibitors. Cancer Cell. 2020;37(4):443-55.

19. Fares CM, Van Allen EM, Drake CG, Allison JP, Hu-Lieskovan S. Mechanisms of Resistance to Immune Checkpoint Blockade: Why Does Checkpoint Inhibitor Immunotherapy Not Work for All Patients? Am Soc Clin Oncol Educ Book. 2019;39:147-64.

20. Borcoman E, Kanjanapan Y, Champiat S, Kato S, Servois V, Kurzrock R, et al. Novel patterns of response under immunotherapy. Ann Oncol. 2019;30(3):385-96.

21. Borcoman E, Nandikolla A, Long G, Goel S, Le Tourneau C. Patterns of Response and Progression to Immunotherapy. Am Soc Clin Oncol Educ Book. 2018;38:169-78.

22. Pons-Tostivint; E, Latouche; A, Vaflard; P, Ricci; F, Loirat; D, Hescot; S, et al. Comparative Analysis of Durable Responses on Immune Checkpoint Inhibitors Versus Other Systemic Therapies: A Pooled Analysis of Phase III Trials. JCO Precision Oncology. 2019;3:1-10.

23. Mansoori B, Mohammadi A, Davudian S, Shirjang S, Baradaran B. The Different Mechanisms of Cancer Drug Resistance: A Brief Review. Adv Pharm Bull. 2017;7(3):339-48.

24. Housman G, Byler S, Heerboth S, Lapinska K, Longacre M, Snyder N, et al. Drug resistance in cancer: an overview. Cancers (Basel). 2014;6(3):1769-92.

25. Groenendijk FH, Bernards R. Drug resistance to targeted therapies: deja vu all over again. Mol Oncol. 2014;8(6):1067-83.

26. Ellis LM, Hicklin DJ. Resistance to Targeted Therapies: Refining Anticancer Therapy in the Era of Molecular Oncology. Clin Cancer Res. 2009;15(24):7471-8.

27. Syn NL, Teng MWL, Mok TSK, Soo RA. De-novo and acquired resistance to immune checkpoint targeting. Lancet Oncol. 2017;18(12):e731-e41.

28. Jenkins RW, Barbie DA, Flaherty KT. Mechanisms of resistance to immune checkpoint inhibitors. Br J Cancer. 2018;118(1):9-16.

29. Zaretsky JM, Garcia-Diaz A, Shin DS, Escuin-Ordinas H, Hugo W, Hu-Lieskovan S, et al. Mutations Associated with Acquired Resistance to PD-1 Blockade in Melanoma. N Engl J Med. 2016;375(9):819-29.

30. Gettinger S, Choi J, Hastings K, Truini A, Datar I, Sowell R, et al. Impaired HLA Class I Antigen Processing and Presentation as a Mechanism of Acquired Resistance to Immune Checkpoint Inhibitors in Lung Cancer. Cancer Discov. 2017;7(12):1420-35.

31. Tran E, Robbins PF, Lu YC, Prickett TD, Gartner JJ, Jia L, et al. T-Cell Transfer Therapy Targeting Mutant KRAS in Cancer. N Engl J Med. 2016;375(23):2255-62.

32. Anagnostou V, Smith KN, Forde PM, Niknafs N, Bhattacharya R, White J, et al. Evolution of Neoantigen Landscape during Immune Checkpoint Blockade in Non-Small Cell Lung Cancer. Cancer Discov. 2017;7(3):264-76.

33. Efremova M, Rieder D, Klepsch V, Charoentong P, Finotello F, Hackl H, et al. Targeting immune checkpoints potentiates immunoediting and changes the dynamics of tumor evolution. Nat Commun. 2018;9(1):32.

34. Koyama S, Akbay EA, Li YY, Herter-Sprie GS, Buczkowski KA, Richards WG, et al. Adaptive resistance to therapeutic PD-1 blockade is associated with upregulation of alternative immune checkpoints. Nat Commun. 2016;7:10501.

35. Gettinger SN, Wurtz A, Goldberg SB, Rimm D, Schalper K, Kaech S, et al. Clinical Features and Management of Acquired Resistance to PD-1 Axis Inhibitors in 26 Patients With Advanced Non-Small Cell Lung Cancer. J Thorac Oncol. 2018;13(6):831-9.

36. Eisenhauer EA, Therasse P, Bogaerts J, Schwartz LH, Sargent D, Ford R, et al. New response evaluation criteria in solid tumours: revised RECIST guideline (version 1.1).

Eur J Cancer. 2009;45(2):228-47.

37. Li H, Durbin R. Fast and accurate long-read alignment with Burrows-Wheeler transform. Bioinformatics. 2010;26(5):589-95.

38. McKenna A, Hanna M, Banks E, Sivachenko A, Cibulskis K, Kernytsky A, et al. The Genome Analysis Toolkit: a MapReduce framework for analyzing next-generation DNA sequencing data. Genome Res. 2010;20(9):1297-303.

39. Wang K, Li M, Hakonarson H. ANNOVAR: functional annotation of genetic variants from high-throughput sequencing data. Nucleic Acids Res. 2010;38(16):e164.

40. Chalmers ZR, Connelly CF, Fabrizio D, Gay L, Ali SM, Ennis R, et al. Analysis of 100,000 human cancer genomes reveals the landscape of tumor mutational burden. Genome Med. 2017;9(1):34.

41. Rosenthal R, McGranahan N, Herrero J, Taylor BS, Swanton C. DeconstructSigs: delineating mutational processes in single tumors distinguishes DNA repair deficiencies and patterns of carcinoma evolution. Genome Biol. 2016;17:31.

42. Gao J, Aksoy BA, Dogrusoz U, Dresdner G, Gross B, Sumer SO, et al. Integrative analysis of complex cancer genomics and clinical profiles using the cBioPortal. Sci Signal. 2013;6(269):pl1.

43. Cerami E, Gao J, Dogrusoz U, Gross BE, Sumer SO, Aksoy BA, et al. The cBio cancer genomics portal: an open platform for exploring multidimensional cancer genomics data. Cancer Discov. 2012;2(5):401-4.

44. D'Aurizio R, Pippucci T, Tattini L, Giusti B, Pellegrini M, Magi A. Enhanced copy number variants detection from whole-exome sequencing data using EXCAVATOR2. Nucleic Acids Res. 2016;44(20):e154.

45. Talevich E, Shain AH, Botton T, Bastian BC. CNVkit: Genome-Wide Copy

Number Detection and Visualization from Targeted DNA Sequencing. PLoS Comput Biol. 2016;12(4):e1004873.

46. Dobin A, Davis CA, Schlesinger F, Drenkow J, Zaleski C, Jha S, et al. STAR: ultrafast universal RNA-seq aligner. Bioinformatics. 2013;29(1):15-21.

47. Li B, Dewey CN. RSEM: accurate transcript quantification from RNA-Seq data with or without a reference genome. BMC Bioinformatics. 2011;12:323.

48. Yoshihara K, Shahmoradgoli M, Martinez E, Vegesna R, Kim H, Torres-Garcia W, et al. Inferring tumour purity and stromal and immune cell admixture from expression data. Nat Commun. 2013;4:2612.

49. Newman AM, Liu CL, Green MR, Gentles AJ, Feng W, Xu Y, et al. Robust enumeration of cell subsets from tissue expression profiles. Nat Methods. 2015;12(5):453-7.

50. Huang da W, Sherman BT, Lempicki RA. Systematic and integrative analysis of large gene lists using DAVID bioinformatics resources. Nat Protoc. 2009;4(1):44-57.

51. Subramanian A, Tamayo P, Mootha VK, Mukherjee S, Ebert BL, Gillette MA, et al. Gene set enrichment analysis: a knowledge-based approach for interpreting genome-wide expression profiles. Proc Natl Acad Sci U S A. 2005;102(43):15545-50.

52. Tate JG, Bamford S, Jubb HC, Sondka Z, Beare DM, Bindal N, et al. COSMIC: the Catalogue Of Somatic Mutations In Cancer. Nucleic Acids Res. 2019;47(D1):D941-D7.

53. Landrum MJ, Lee JM, Benson M, Brown G, Chao C, Chitipiralla S, et al. ClinVar: public archive of interpretations of clinically relevant variants. Nucleic Acids Res. 2016;44(D1):D862-8.

54. Chakravarty D, Gao J, Phillips SM, Kundra R, Zhang H, Wang J, et al. OncoKB: A Precision Oncology Knowledge Base. JCO Precis Oncol. 2017;2017.

55. Liu Y, He M, Wang D, Diao L, Liu J, Tang L, et al. HisgAtlas 1.0: a human

immunosuppression gene database. Database (Oxford). 2017;2017.

56. Rooney MS, Shukla SA, Wu CJ, Getz G, Hacohen N. Molecular and genetic properties of tumors associated with local immune cytolytic activity. Cell. 2015;160(1-2):48-61.

57. Kanehisa M, Goto S. KEGG: kyoto encyclopedia of genes and genomes. Nucleic Acids Res. 2000;28(1):27-30.

58. Gao J, Shi LZ, Zhao H, Chen J, Xiong L, He Q, et al. Loss of IFN-gamma Pathway Genes in Tumor Cells as a Mechanism of Resistance to Anti-CTLA-4 Therapy. Cell. 2016;167(2):397-404 e9.

59. Ayers M, Lunceford J, Nebozhyn M, Murphy E, Loboda A, Kaufman DR, et al. IFN-gamma-related mRNA profile predicts clinical response to PD-1 blockade. J Clin Invest. 2017;127(8):2930-40.

60. Pai CS, Huang JT, Lu X, Simons DM, Park C, Chang A, et al. Clonal Deletion of Tumor-Specific T Cells by Interferon-gamma Confers Therapeutic Resistance to Combination Immune Checkpoint Blockade. Immunity. 2019;50(2):477-92 e8.

61. Rizvi NA, Hellmann MD, Snyder A, Kvistborg P, Makarov V, Havel JJ, et al. Cancer immunology. Mutational landscape determines sensitivity to PD-1 blockade in non-small cell lung cancer. Science. 2015;348(6230):124-8.

62. Le DT, Durham JN, Smith KN, Wang H, Bartlett BR, Aulakh LK, et al. Mismatch repair deficiency predicts response of solid tumors to PD-1 blockade. Science. 2017;357(6349):409-13.

63. Diaz LA, Jr., Le DT. PD-1 Blockade in Tumors with Mismatch-Repair Deficiency. N Engl J Med. 2015;373(20):1979.

64. Chen H, Chong W, Teng C, Yao Y, Wang X, Li X. The immune response-related

mutational signatures and driver genes in non-small-cell lung cancer. Cancer Sci. 2019;110(8):2348-56.

65. Alexandrov LB, Nik-Zainal S, Wedge DC, Aparicio SA, Behjati S, Biankin AV, et al. Signatures of mutational processes in human cancer. Nature. 2013;500(7463):415-21.

66. Zhang Y, Kwok-Shing Ng P, Kucherlapati M, Chen F, Liu Y, Tsang YH, et al. A Pan-Cancer Proteogenomic Atlas of PI3K/AKT/mTOR Pathway Alterations. Cancer Cell. 2017;31(6):820-32 e3.

67. Cretella D, Digiacomo G, Giovannetti E, Cavazzoni A. PTEN Alterations as a Potential Mechanism for Tumor Cell Escape from PD-1/PD-L1 Inhibition. Cancers (Basel). 2019;11(9).

68. George S, Miao D, Demetri GD, Adeegbe D, Rodig SJ, Shukla S, et al. Loss of PTEN Is Associated with Resistance to Anti-PD-1 Checkpoint Blockade Therapy in Metastatic Uterine Leiomyosarcoma. Immunity. 2017;46(2):197-204.

69. Trujillo JA, Luke JJ, Zha Y, Segal JP, Ritterhouse LL, Spranger S, et al. Secondary resistance to immunotherapy associated with beta-catenin pathway activation or PTEN loss in metastatic melanoma. J Immunother Cancer. 2019;7(1):295.

70. Peng W, Chen JQ, Liu C, Malu S, Creasy C, Tetzlaff MT, et al. Loss of PTEN Promotes Resistance to T Cell-Mediated Immunotherapy. Cancer Discov. 2016;6(2):202-16.

71. Roberts SA, Lawrence MS, Klimczak LJ, Grimm SA, Fargo D, Stojanov P, et al. An APOBEC cytidine deaminase mutagenesis pattern is widespread in human cancers. Nat Genet. 2013;45(9):970-6.

72. Nik-Zainal S, Alexandrov LB, Wedge DC, Van Loo P, Greenman CD, Raine K, et al. Mutational processes molding the genomes of 21 breast cancers. Cell. 2012;149(5):979-93.

73. Morsalin S, Yang C, Fang J, Reddy S, Kayarthodi S, Childs E, et al. Molecular Mechanism of beta-Catenin Signaling Pathway Inactivation in ETV1-Positive Prostate Cancers. J Pharm Sci Pharmacol. 2015;2(3):208-16.

74. Jho EH, Zhang T, Domon C, Joo CK, Freund JN, Costantini F. Wnt/beta-catenin/Tcf signaling induces the transcription of Axin2, a negative regulator of the signaling pathway. Mol Cell Biol. 2002;22(4):1172-83.

75. Luke JJ, Bao R, Sweis RF, Spranger S, Gajewski TF. WNT/beta-catenin Pathway Activation Correlates with Immune Exclusion across Human Cancers. Clin Cancer Res. 2019;25(10):3074-83.

76. Xu YP, Lv L, Liu Y, Smith MD, Li WC, Tan XM, et al. Tumor suppressor TET2 promotes cancer immunity and immunotherapy efficacy. J Clin Invest. 2019;130:4316-31.

77. Cottrell TR, Taube JM. PD-L1 and Emerging Biomarkers in Immune Checkpoint Blockade Therapy. Cancer J. 2018;24(1):41-6.

78. Erlmeier F, Weichert W, Schrader AJ, Autenrieth M, Hartmann A, Steffens S, et al. Prognostic impact of PD-1 and its ligands in renal cell carcinoma. Med Oncol. 2017;34(6):99.

79. Zhu J, Armstrong AJ, Friedlander TW, Kim W, Pal SK, George DJ, et al. Biomarkers of immunotherapy in urothelial and renal cell carcinoma: PD-L1, tumor mutational burden, and beyond. J Immunother Cancer. 2018;6(1):4.

80. Takahashi T, Tateishi A, Bychkov A, Fukuoka J. Remarkable Alteration of PD-L1 Expression after Immune Checkpoint Therapy in Patients with Non-Small-Cell Lung Cancer: Two Autopsy Case Reports. Int J Mol Sci. 2019;20(10).

81. Haratake N, Toyokawa G, Tagawa T, Kozuma Y, Matsubara T, Takamori S, et al. Positive Conversion of PD-L1 Expression After Treatments with Chemotherapy and

Nivolumab. Anticancer Res. 2017;37(10):5713-7.

82. Uryvaev A, Passhak M, Hershkovits D, Sabo E, Bar-Sela G. The role of tumor-infiltrating lymphocytes (TILs) as a predictive biomarker of response to anti-PD1 therapy in patients with metastatic non-small cell lung cancer or metastatic melanoma. Med Oncol. 2018;35(3):25.

83. Chen PL, Roh W, Reuben A, Cooper ZA, Spencer CN, Prieto PA, et al. Analysis of Immune Signatures in Longitudinal Tumor Samples Yields Insight into Biomarkers of Response and Mechanisms of Resistance to Immune Checkpoint Blockade. Cancer Discov. 2016;6(8):827-37.

84. Pardoll DM. The blockade of immune checkpoints in cancer immunotherapy. Nat Rev Cancer. 2012;12(4):252-64.

85. Rotte A, Jin JY, Lemaire V. Mechanistic overview of immune checkpoints to support the rational design of their combinations in cancer immunotherapy. Ann Oncol. 2018;29(1):71-83.

86. Xu W, Dong J, Zheng Y, Zhou J, Yuan Y, Ta HM, et al. Immune-Checkpoint Protein VISTA Regulates Antitumor Immunity by Controlling Myeloid Cell-Mediated Inflammation and Immunosuppression. Cancer Immunol Res. 2019;7(9):1497-510.

87. Arce Vargas F, Furness AJS, Solomon I, Joshi K, Mekkaoui L, Lesko MH, et al. Fc-Optimized Anti-CD25 Depletes Tumor-Infiltrating Regulatory T Cells and Synergizes with PD-1 Blockade to Eradicate Established Tumors. Immunity. 2017;46(4):577-86.

88. Zer A, Sung MR, Walia P, Khoja L, Maganti M, Labbe C, et al. Correlation of Neutrophil to Lymphocyte Ratio and Absolute Neutrophil Count With Outcomes With PD-1 Axis Inhibitors in Patients With Advanced Non-Small-Cell Lung Cancer. Clin Lung Cancer. 2018;19(5):426-34 e1.

89. Tan Q, Liu S, Liang C, Han X, Shi Y. Pretreatment hematological markers predict clinical outcome in cancer patients receiving immune checkpoint inhibitors: A meta-analysis. Thorac Cancer. 2018;9(10):1220-30.

90. Vano YA, Oudard S, By MA, Tetu P, Thibault C, Aboudagga H, et al. Optimal cut-off for neutrophil-to-lymphocyte ratio: Fact or Fantasy? A prospective cohort study in metastatic cancer patients. PLoS One. 2018;13(4):e0195042.

91. Bagley SJ, Kothari S, Aggarwal C, Bauml JM, Alley EW, Evans TL, et al. Pretreatment neutrophil-to-lymphocyte ratio as a marker of outcomes in nivolumab-treated patients with advanced non-small-cell lung cancer. Lung Cancer. 2017;106:1-7.

92. Ferrucci PF, Gandini S, Battaglia A, Alfieri S, Di Giacomo AM, Giannarelli D, et al. Baseline neutrophil-to-lymphocyte ratio is associated with outcome of ipilimumab-treated metastatic melanoma patients. Br J Cancer. 2015;112(12):1904-10.

93. Capone M, Giannarelli D, Mallardo D, Madonna G, Festino L, Grimaldi AM, et al. Baseline neutrophil-to-lymphocyte ratio (NLR) and derived NLR could predict overall survival in patients with advanced melanoma treated with nivolumab. J Immunother Cancer. 2018;6(1):74.

94. Diem S, Kasenda B, Spain L, Martin-Liberal J, Marconcini R, Gore M, et al. Serum lactate dehydrogenase as an early marker for outcome in patients treated with anti-PD-1 therapy in metastatic melanoma. Br J Cancer. 2016;114(3):256-61.

95. Paulson KG, Voillet V, McAfee MS, Hunter DS, Wagener FD, Perdicchio M, et al. Acquired cancer resistance to combination immunotherapy from transcriptional loss of class I HLA. Nat Commun. 2018;9(1):3868.

96. Benci JL, Xu B, Qiu Y, Wu TJ, Dada H, Twyman-Saint Victor C, et al. Tumor Interferon Signaling Regulates a Multigenic Resistance Program to Immune Checkpoint

Blockade. Cell. 2016;167(6):1540-54 e12.

97. Kobayashi Y, Lim SO, Yamaguchi H. Oncogenic signaling pathways associated with immune evasion and resistance to immune checkpoint inhibitors in cancer. Semin Cancer Biol. 2019.

98. Sanchez-Vega F, Mina M, Armenia J, Chatila WK, Luna A, La KC, et al. Oncogenic Signaling Pathways in The Cancer Genome Atlas. Cell. 2018;173(2):321-37 e10.

99. Parsa AT, Waldron JS, Panner A, Crane CA, Parney IF, Barry JJ, et al. Loss of tumor suppressor PTEN function increases B7-H1 expression and immunoresistance in glioma. Nat Med. 2007;13(1):84-8.

100. Crane CA, Panner A, Murray JC, Wilson SP, Xu H, Chen L, et al. PI(3) kinase is associated with a mechanism of immunoresistance in breast and prostate cancer. Oncogene. 2009;28(2):306-12.

101. Lastwika KJ, Wilson W, 3rd, Li QK, Norris J, Xu H, Ghazarian SR, et al. Control of PD-L1 Expression by Oncogenic Activation of the AKT-mTOR Pathway in Non-Small Cell Lung Cancer. Cancer Res. 2016;76(2):227-38.

102. Borcoman E, De La Rochere P, Richer W, Vacher S, Chemlali W, Krucker C, et al. Inhibition of PI3K pathway increases immune infiltrate in muscle-invasive bladder cancer. Oncoimmunology. 2019;8(5):e1581556.

103. Davis RJ, Moore EC, Clavijo PE, Friedman J, Cash H, Chen Z, et al. Anti-PD-L1 Efficacy Can Be Enhanced by Inhibition of Myeloid-Derived Suppressor Cells with a Selective Inhibitor of PI3Kdelta/gamma. Cancer Res. 2017;77(10):2607-19.

104. Kaneda MM, Messer KS, Ralainirina N, Li H, Leem CJ, Gorjestani S, et al. PI3Kgamma is a molecular switch that controls immune suppression. Nature. 2016;539(7629):437-42.

105. Smith NJ, Fenton TR. The APOBEC3 genes and their role in cancer: insights from human papillomavirus. J Mol Endocrinol. 2019.

106. Alexandrov LB, Nik-Zainal S, Wedge DC, Campbell PJ, Stratton MR. Deciphering signatures of mutational processes operative in human cancer. Cell Rep. 2013;3(1):246-59.

107. Henderson S, Chakravarthy A, Su X, Boshoff C, Fenton TR. APOBEC-mediated cytosine deamination links PIK3CA helical domain mutations to human papillomavirus-driven tumor development. Cell Rep. 2014;7(6):1833-41.

108. Barroso-Sousa R, Jain E, Cohen O, Kim D, Buendia-Buendia J, Winer E, et al. Prevalence and mutational determinants of high tumor mutation burden in breast cancer. Ann Oncol. 2020;31(3):387-94.

109. Boichard A, Pham TV, Yeerna H, Goodman A, Tamayo P, Lippman S, et al. APOBEC-related mutagenesis and neo-peptide hydrophobicity: implications for response to immunotherapy. Oncoimmunology. 2019;8(3):1550341.

110. Wang S, Jia M, He Z, Liu XS. APOBEC3B and APOBEC mutational signature as potential predictive markers for immunotherapy response in non-small cell lung cancer. Oncogene. 2018;37(29):3924-36.

111. Lui VW, Hedberg ML, Li H, Vangara BS, Pendleton K, Zeng Y, et al. Frequent mutation of the PI3K pathway in head and neck cancer defines predictive biomarkers. Cancer Discov. 2013;3(7):761-9.

112. Lechner M, Frampton GM, Fenton T, Feber A, Palmer G, Jay A, et al. Targeted next-generation sequencing of head and neck squamous cell carcinoma identifies novel genetic alterations in HPV+ and HPV- tumors. Genome Med. 2013;5(5):49.

113. Ruiz de Galarreta M, Bresnahan E, Molina-Sanchez P, Lindblad KE, Maier B, Sia

D, et al. beta-Catenin Activation Promotes Immune Escape and Resistance to Anti-PD-1 Therapy in Hepatocellular Carcinoma. Cancer Discov. 2019;9(8):1124-41.

114. Spranger S, Bao R, Gajewski TF. Melanoma-intrinsic beta-catenin signalling prevents anti-tumour immunity. Nature. 2015;523(7559):231-5.

115. Gorgoulis V, Adams PD, Alimonti A, Bennett DC, Bischof O, Bishop C, et al. Cellular Senescence: Defining a Path Forward. Cell. 2019;179(4):813-27.

116. Huang RY, Francois A, McGray AR, Miliotto A, Odunsi K. Compensatory upregulation of PD-1, LAG-3, and CTLA-4 limits the efficacy of single-agent checkpoint blockade in metastatic ovarian cancer. Oncoimmunology. 2017;6(1):e1249561.

117. Johnson DB, Nixon MJ, Wang Y, Wang DY, Castellanos E, Estrada MV, et al. Tumor-specific MHC-II expression drives a unique pattern of resistance to immunotherapy via LAG-3/FCRL6 engagement. JCI Insight. 2018;3(24).

118. Shayan G, Srivastava R, Li J, Schmitt N, Kane LP, Ferris RL. Adaptive resistance to anti-PD1 therapy by Tim-3 upregulation is mediated by the PI3K-Akt pathway in head and neck cancer. Oncoimmunology. 2017;6(1):e1261779.

119. Gide TN, Wilmott JS, Scolyer RA, Long GV. Primary and Acquired Resistance to Immune Checkpoint Inhibitors in Metastatic Melanoma. Clin Cancer Res. 2018;24(6):1260-70.

120. Taube JM, Young GD, McMiller TL, Chen S, Salas JT, Pritchard TS, et al. Differential Expression of Immune-Regulatory Genes Associated with PD-L1 Display in Melanoma: Implications for PD-1 Pathway Blockade. Clin Cancer Res. 2015;21(17):3969-76.

121. Saleh R, Elkord E. Acquired resistance to cancer immunotherapy: Role of tumor-mediated immunosuppression. Semin Cancer Biol. 2019.

122. Cassetta L, Kitamura T. Macrophage targeting: opening new possibilities for cancer immunotherapy. Immunology. 2018;155(3):285-93.

123. Saleh R, Elkord E. Treg-mediated acquired resistance to immune checkpoint inhibitors. Cancer Lett. 2019;457:168-79.

124. Yang L, Lin PC. Mechanisms that drive inflammatory tumor microenvironment, tumor heterogeneity, and metastatic progression. Semin Cancer Biol. 2017;47:185-95.

국문 초록

면역관문억제제에 대한 내성 획득 시 유전체, 전사체 및 병리학적 변화에 대한 통합적 분석

서론: 면역관문억제제는 여러 암종에서 떠오르는 역할을 하고 있다. 면역관문억제제로 치료받은 환자들의 일부에서 장기간 치료 반응이 유지되지만 결과적으로 암이 진행하며 면역관문억제제에 대한 획득 내성을 보인다. 그러나 아직 획득 내성 기전은 잘 알려지지 않았다. 본 연구에서는 면역관문억제제 치료 전후의 유전체, 전사체 및 병리학적 변화를 종양 내적 측면과 종양 외적(면역) 측면에서 통합적으로 보고자, 면역관문억제제에 대해 반응한 이후 획득 내성을 경험한 환자들의 면역관문억제제 치료 전후 암조직을 분석하였다.

방법: 2013년 12월부터 2017년 6월까지 서울대학교병원에서 면역관문억제제를 투여 받은 면역학적 암종 (신세포암, 요로상피세포암 및 두경부암) 환자들을 후향적으로 분석하였다. 면역관문억제제에 대해 반응 (완전반응, 부분 반응, 혹은 6개월 이상의 안정 병변)을 보인 후 진행하였고, 분석 가능한 포르말린 고정 파라핀 조직이 있는 경우 연구에 포함되었다. 치료 전과 치료 후 내성 조직에 대하여 엑솜시퀀싱 (whole exome

sequencing), RNA 시퀀싱 및 다중 면역화학염색 (multiplex immunohistochemistry)를 시행하였다. 암 돌연변이 부담, 돌연변이 원(mutation signature) 및 획득 내성과 관련된 체성 돌연변이를 조사하였다. 면역세포 침윤, 면역관문 및 면역 활성 인자와 같은 면역 관련 인자들, 종양 미세환경의 구성요소를 분석하였다. 평가된 인자들은 종양 내적 요인 및 종양 외적 요인으로(국소 면역, 전신 면역) 나누어 분류되었다.

결과: 본 연구는 총 6명의 환자에 대해 분석을 하였다. 획득 내성 발생까지의 기간은 중앙값 370일 (범위, 210일 – 739일)이었다. 첫번째 환자는 인유두종 바이러스 양성인 두경부 편평세포암 환자로, 치료 전후 암조직에서 뚜렷한 APOBEC 관련 돌연변이원을 보였다. 이 환자의 내성 시점 암 조직에서는 *PIK3CA* 유전자에 missense mutation인 E542K가 발생하였는데, 이는 PI3K-Akt 신호전달 경로를 활성화시킬 수 있고 획득 내성을 야기할 수도 있다. 이 환자에서는 치료 후 내성 시점에서 종양 돌연변이 부담이 증가한 반면, 세포독성 CD8 양성 T 세포와 *PD-1*, *LAG3*, *TIM3*와 같은 면역관문의 발현은 내성을 획득하는 동안 모두 감소하는 것을 보였다. 반면, 두번째 환자의 다중 면역화학염색과 RNA 시퀀싱 결과에서 치료 전에 비해 치료 후 조직에서 CD8 양성 종양침윤 림프구뿐만 아니라 *PD-1*, *LAG3*, *TIM3*을 포함하는 면역억제성 인자들의 발현이 높게 나타나는 것을 확인하였다. 세번째 환자는 *AXIN2* 유전자에

stop-gain mutation이, 네번째 환자는 *TET2* 유전자에 frameshift deletion mutation이 발생하였다. 전체 환자에서 항원 제시 구성 요소 혹은 인터페론 감마 관련 경로에 대한 의미 있는 돌연변이나 복제 수 이상은 발견되지 않았다.

결론: 본 연구에서는 면역관문억제제 치료 후 내성을 획득한 시점에서 면역억제성 인자들의 상승이 관찰되었다. APOBEC에 의해 매개되는 *PIK3CA* 돌연변이 발생 과정은 획득 내성에 대한 잠재적인 기전이 될 수 있다.

주요어: 획득 내성, 기전, 면역관문억제제, 차세대 염기서열 분석, 면역화학염색, Programmed death-ligand 1, PIK3CA

학번: 2017-31850